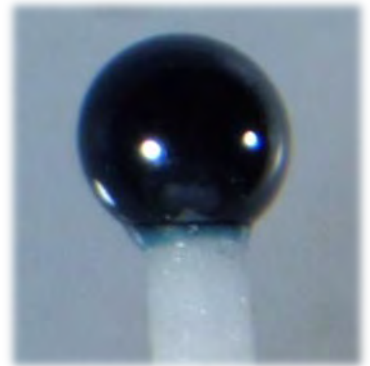


Quantum magnonics with a macroscopic ferromagnetic sphere

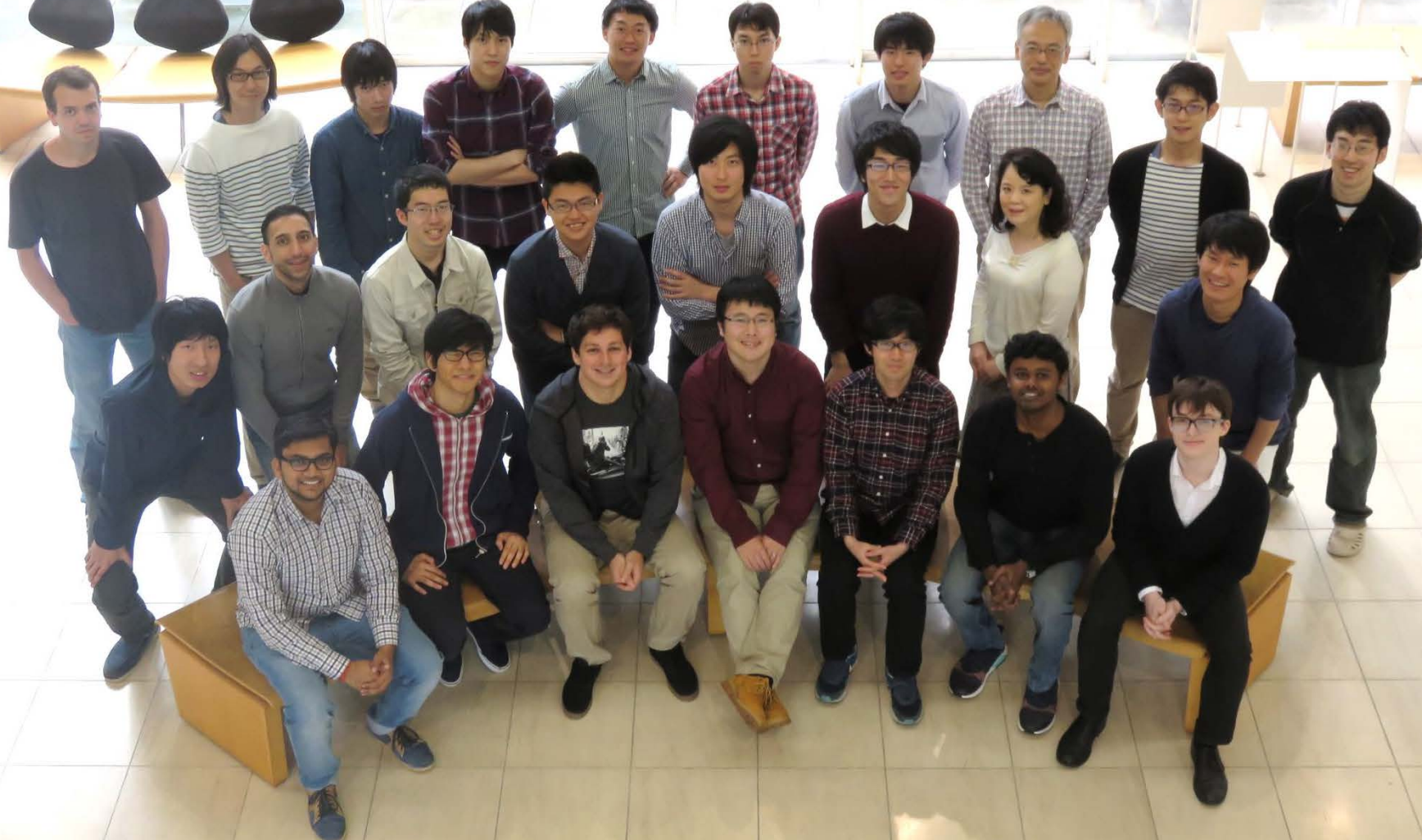
Yasunobu Nakamura

Superconducting Quantum Electronics Team
Center for Emergent Matter Science (CEMS), RIKEN

Research Center for Advanced Science and Technology (RCAST),
The University of Tokyo



Quantum Information Physics & Engineering Lab @ UTokyo



<http://www.qc.rcast.u-tokyo.ac.jp/>

The magnonists

Ryosuke Mori



Seiichiro Ishino



Dany
Lachance-Quirion
(Sherbrooke)

Yutaka Tabuchi



Alto Osada



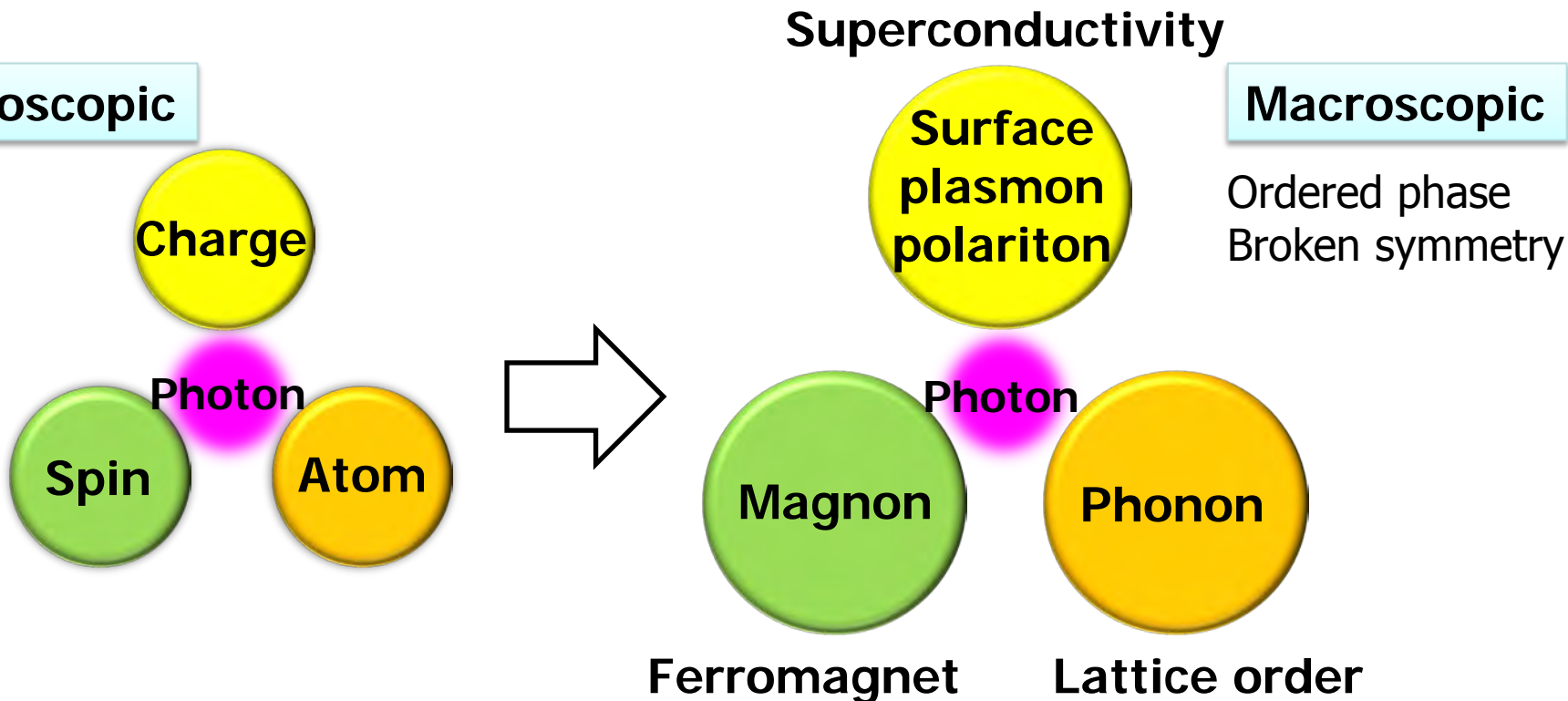
Koji Usami



Ryusuke Hisatomi

Quantum mechanics in macroscopic scale

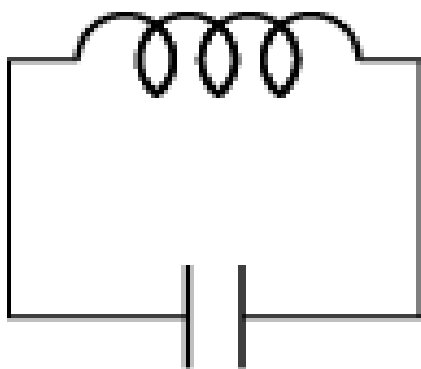
Quantum state control of collective excitation modes in solids



- Spatially-extended rigid mode
- Large transition moment

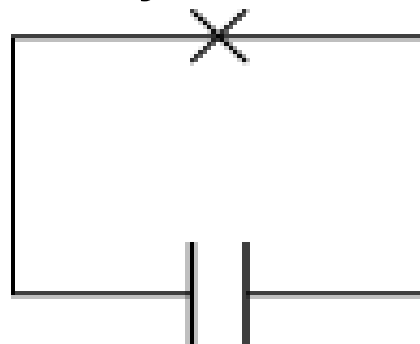
Superconducting qubit – nonlinear resonator

LC resonator



Josephson junction resonator

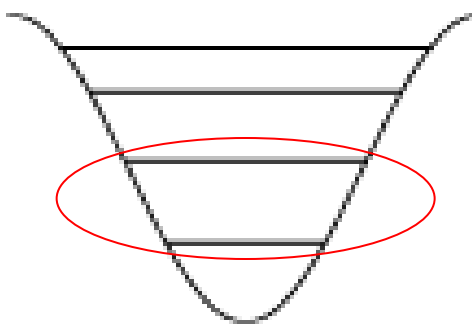
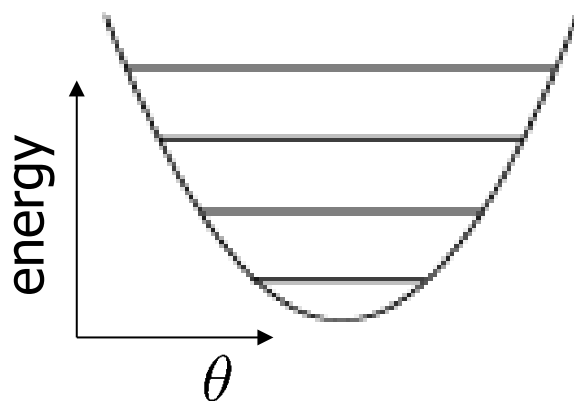
Josephson junction = nonlinear inductor



0.5 μm

0.5 mm

anharmonicity \Rightarrow effective two-level system

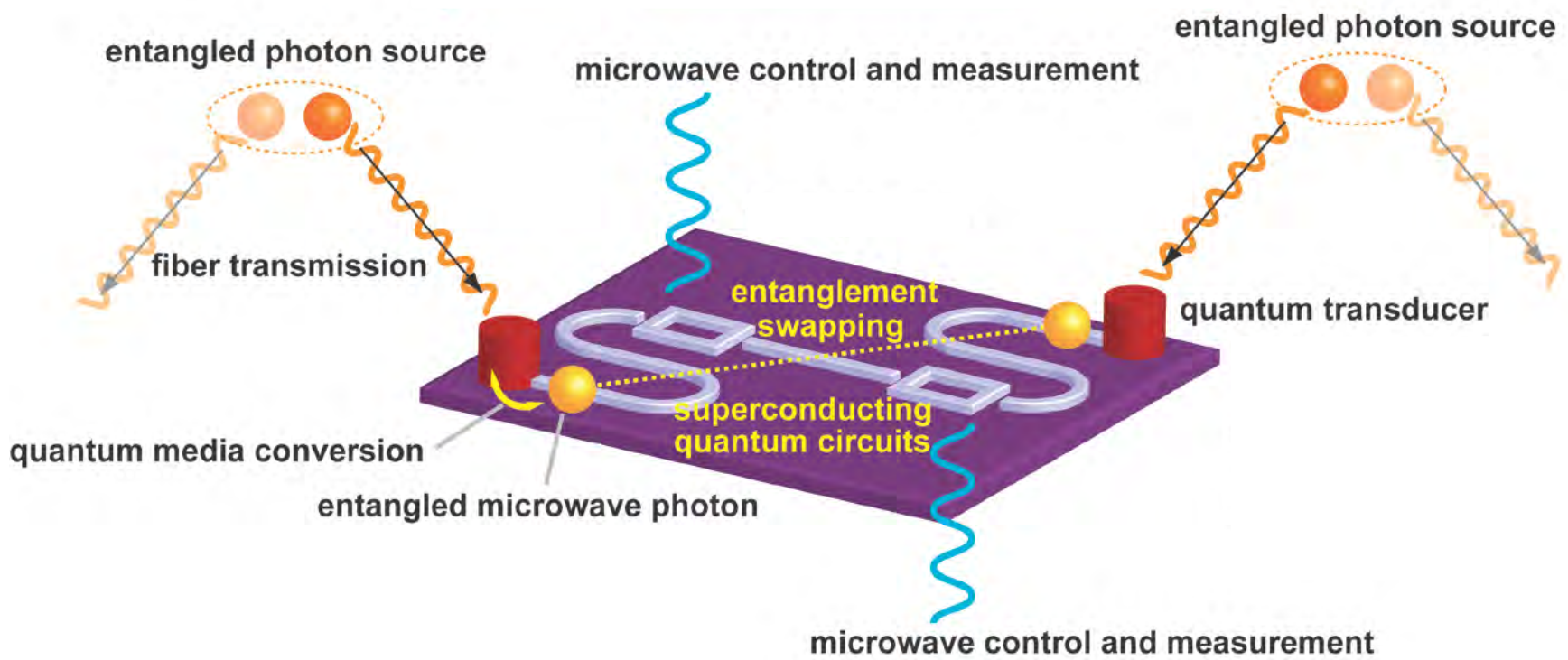


inductive energy = confinement potential

charging energy = kinetic energy \Rightarrow quantized states

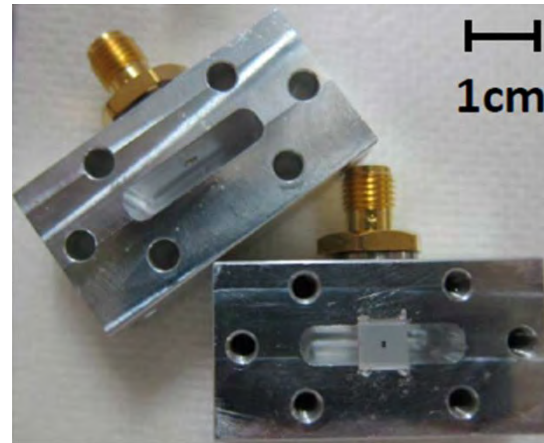
Quantum interface between microwave and light

- Quantum repeater
- Quantum computing network



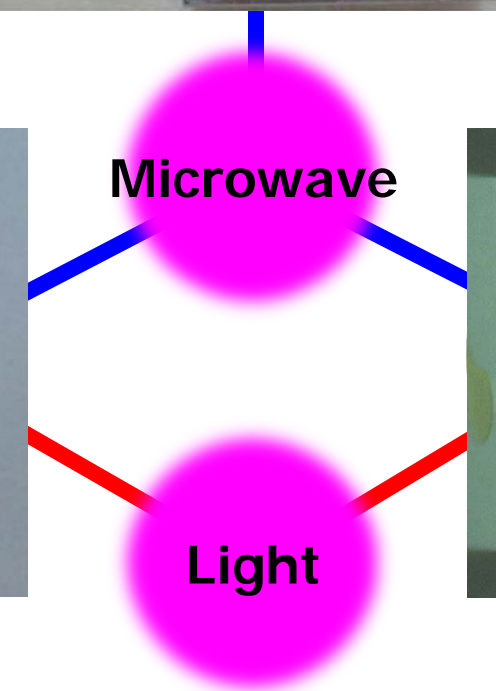
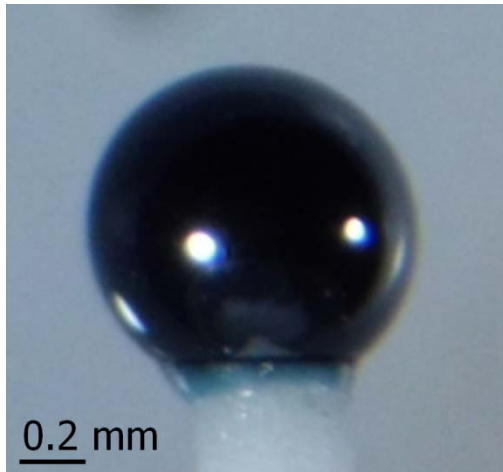
Hybrid quantum systems

Superconducting quantum electronics

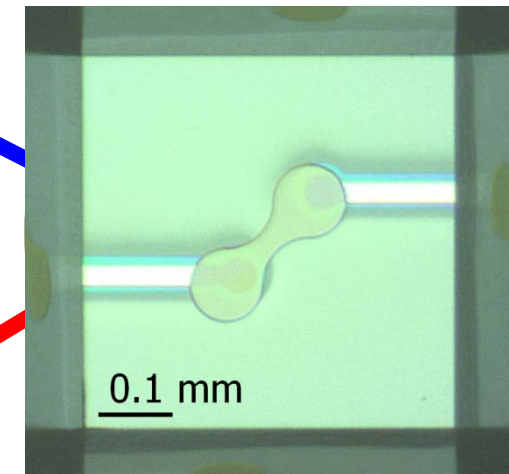


Nonlinearity

Quantum
magnonics



Quantum
nanomechanics

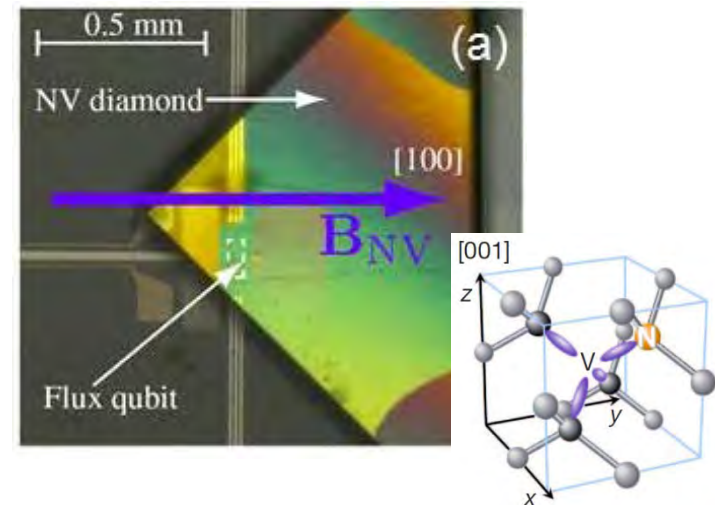
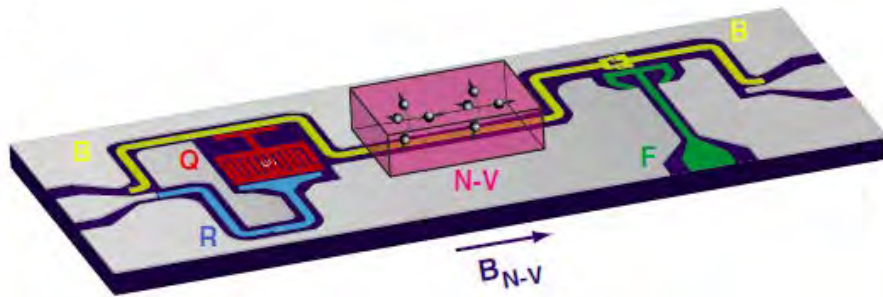


Quantum
surface acoustics

Quantum magnonics

Hybrid with paramagnetic spin ensembles

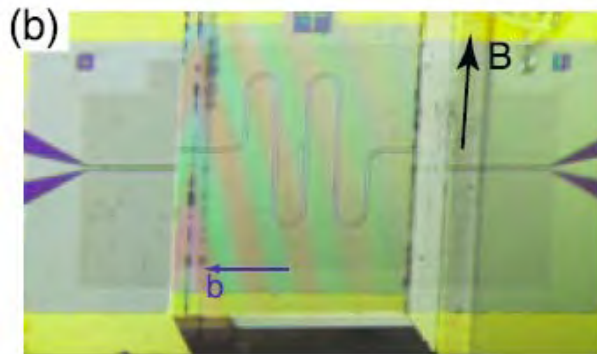
Spin ensemble of NV-centers in diamond



Kubo et al. PRL 107, 220501 (2011). CEA Saclay
R. Amsüss et al. PRL 107 060502 (2011). TUWien

Zhu et al. Nature 478, 221 (2011). (NTT)
Saito et al. Phys. Rev. Lett. 111, 107008 (2013). (NTT)

Rare-earth doped crystal



Optical quantum memory

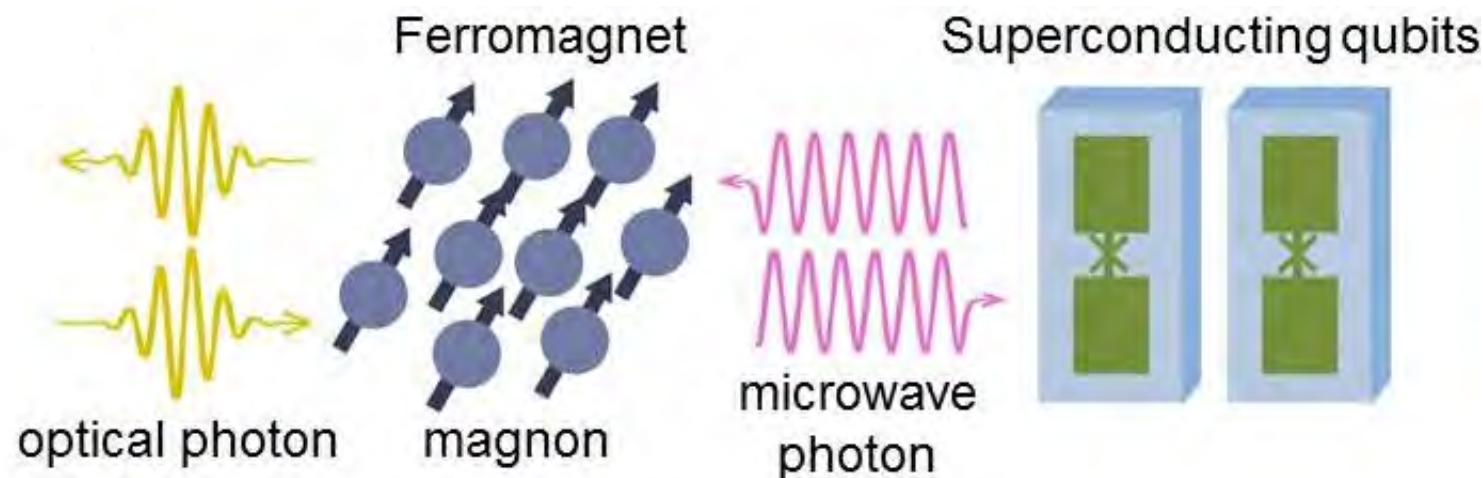
Bushev et al. PRB 84, 060501(R) (2011) Karlsruhe



Hedges et al. Nature 465, 1052 (2010) Otago



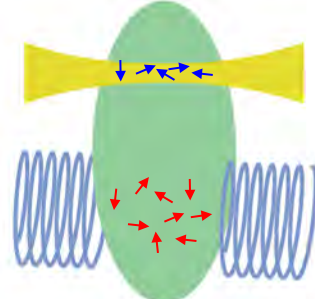
Hybrid with ferromagnetic magnons



Paramagnet

Low spin density 10^{12} - 10^{18} cm^{-3}
Spatial mode defined by EM fields

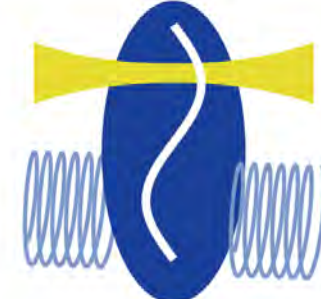
Optical Light



Ferromagnet

High spin density 10^{21} - 10^{22} cm^{-3}
Robust extended spatial mode

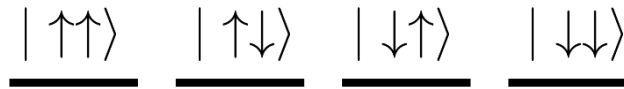
Optical Light



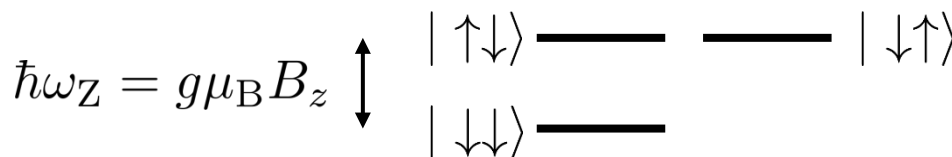
Two coupled spins

$$H = -g\mu_B B_z S_z - 2J\mathbf{S}_1 \cdot \mathbf{S}_2$$

$$B_z = 0, J = 0$$

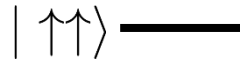


$$B_z \neq 0, J = 0$$



$$B_z \neq 0, J \neq 0$$

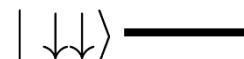
2-magnon



1-magnon



0-magnon



$$|\uparrow\downarrow\rangle - |\downarrow\uparrow\rangle$$

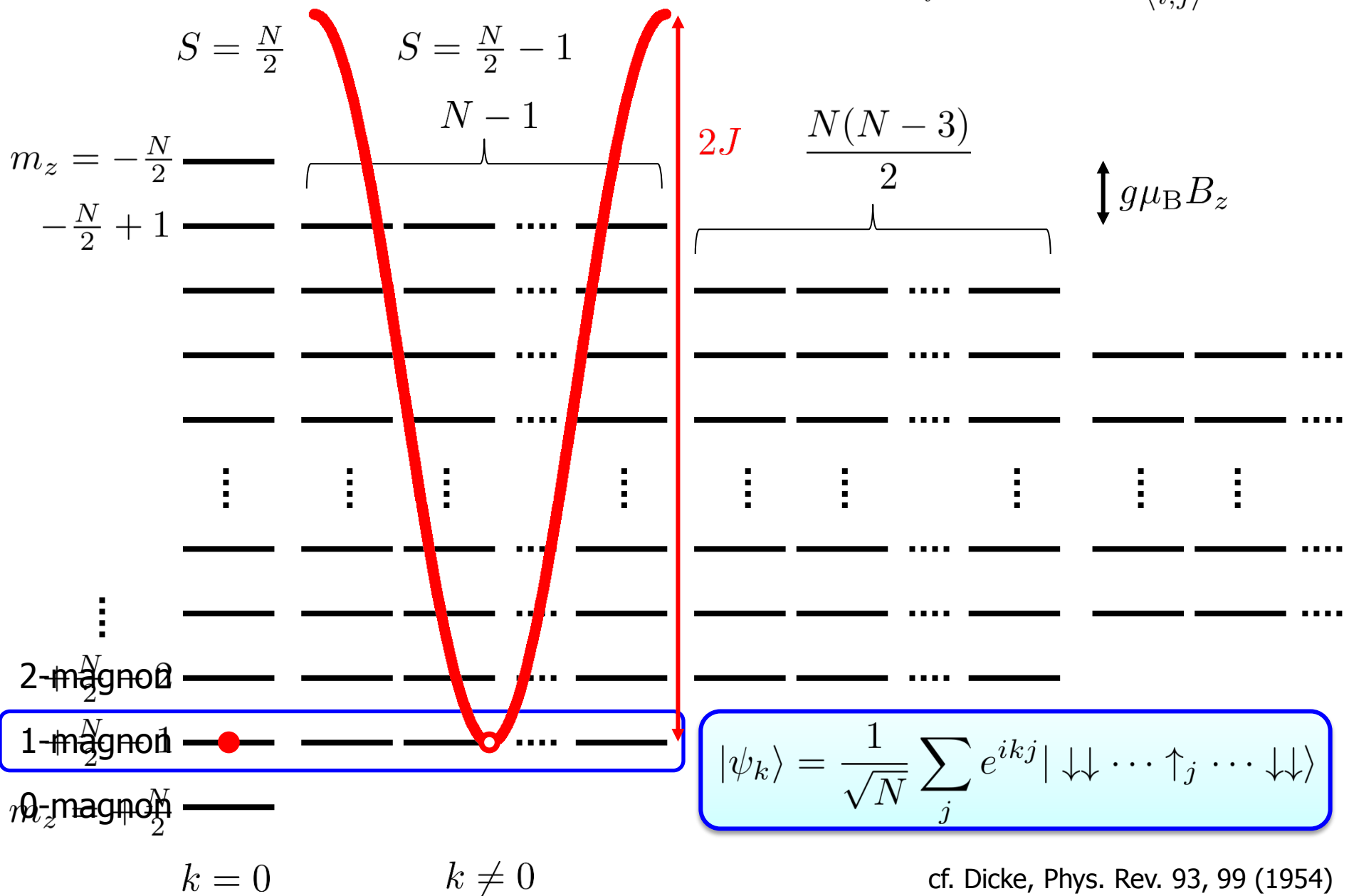
$$2J$$

$$k = 0$$

$$k \neq 0$$

N coupled spins

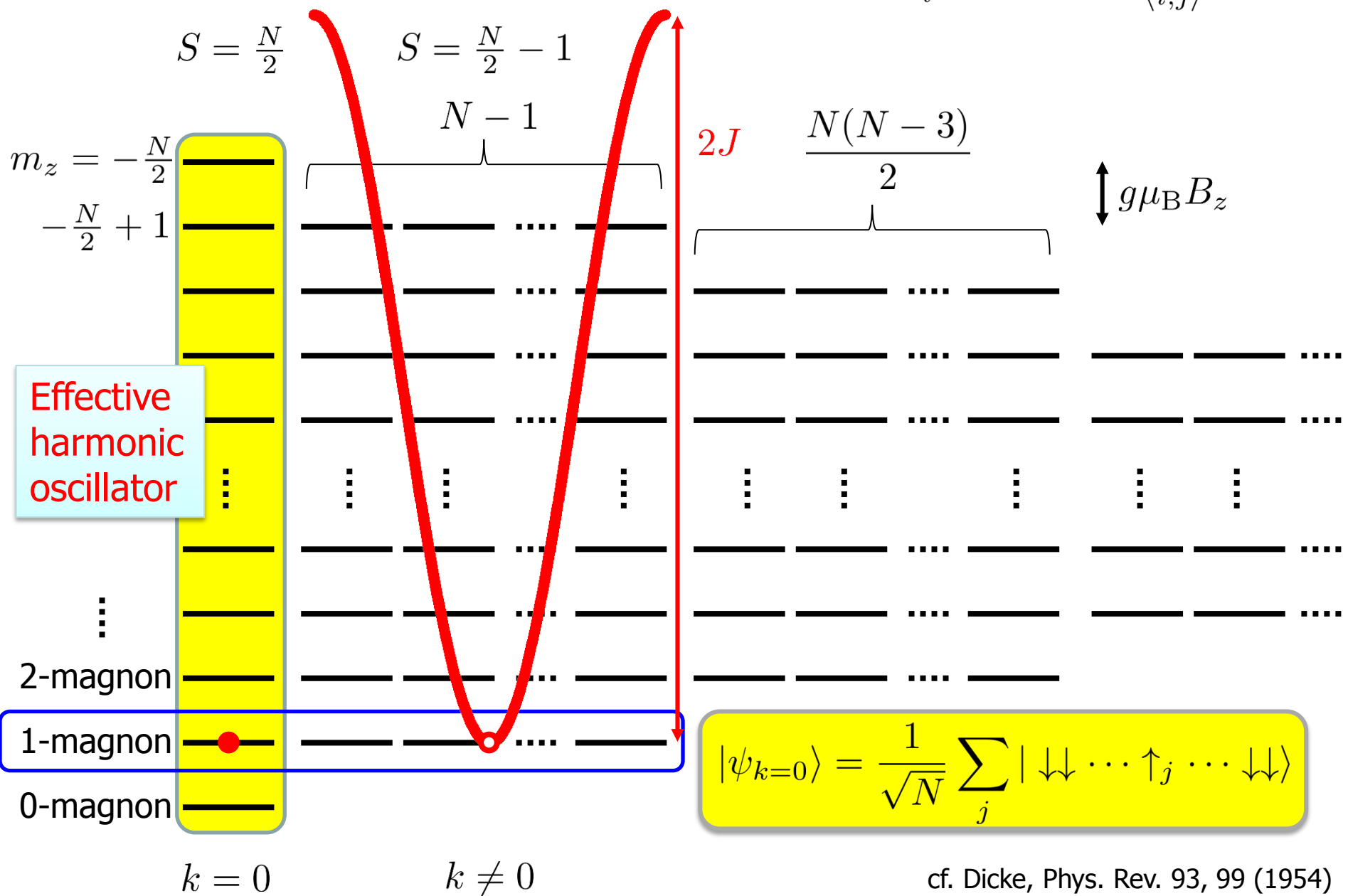
$$H = -g\mu_B \sum_i B_z S_z^i - 2J \sum_{\langle i,j \rangle} \mathbf{S}_i \cdot \mathbf{S}_j$$



cf. Dicke, Phys. Rev. 93, 99 (1954)

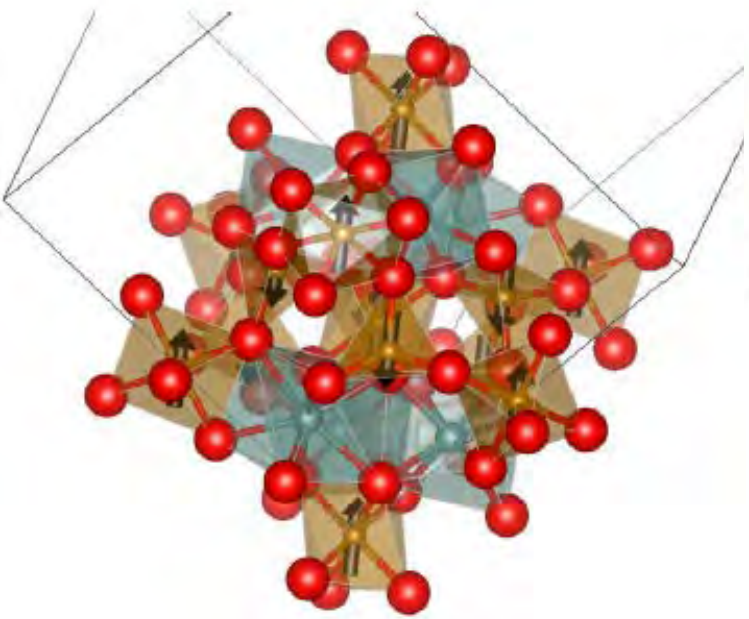
N coupled spins

$$H = -g\mu_B \sum_i B_z S_z^i - 2J \sum_{\langle i,j \rangle} \mathbf{S}_i \cdot \mathbf{S}_j$$



cf. Dicke, Phys. Rev. 93, 99 (1954)

Yttrium Iron Garnet (YIG)



● : O²⁻
● : Fe³⁺
● : Y³⁺
→ : spin
 $5\mu_B$

- Ferrimagnetic **insulator**
- Narrow FMR line
- Transparent at infrared
- High Curie temperature: ~550 K
- Large spin density: $2.1 \times 10^{22} \text{ cm}^{-3}$

Microwave oscillators



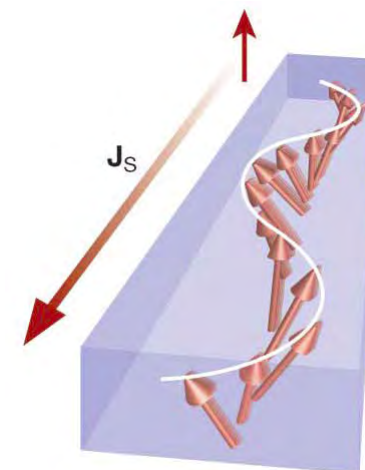
CANDOX Corporation

Optical isolators



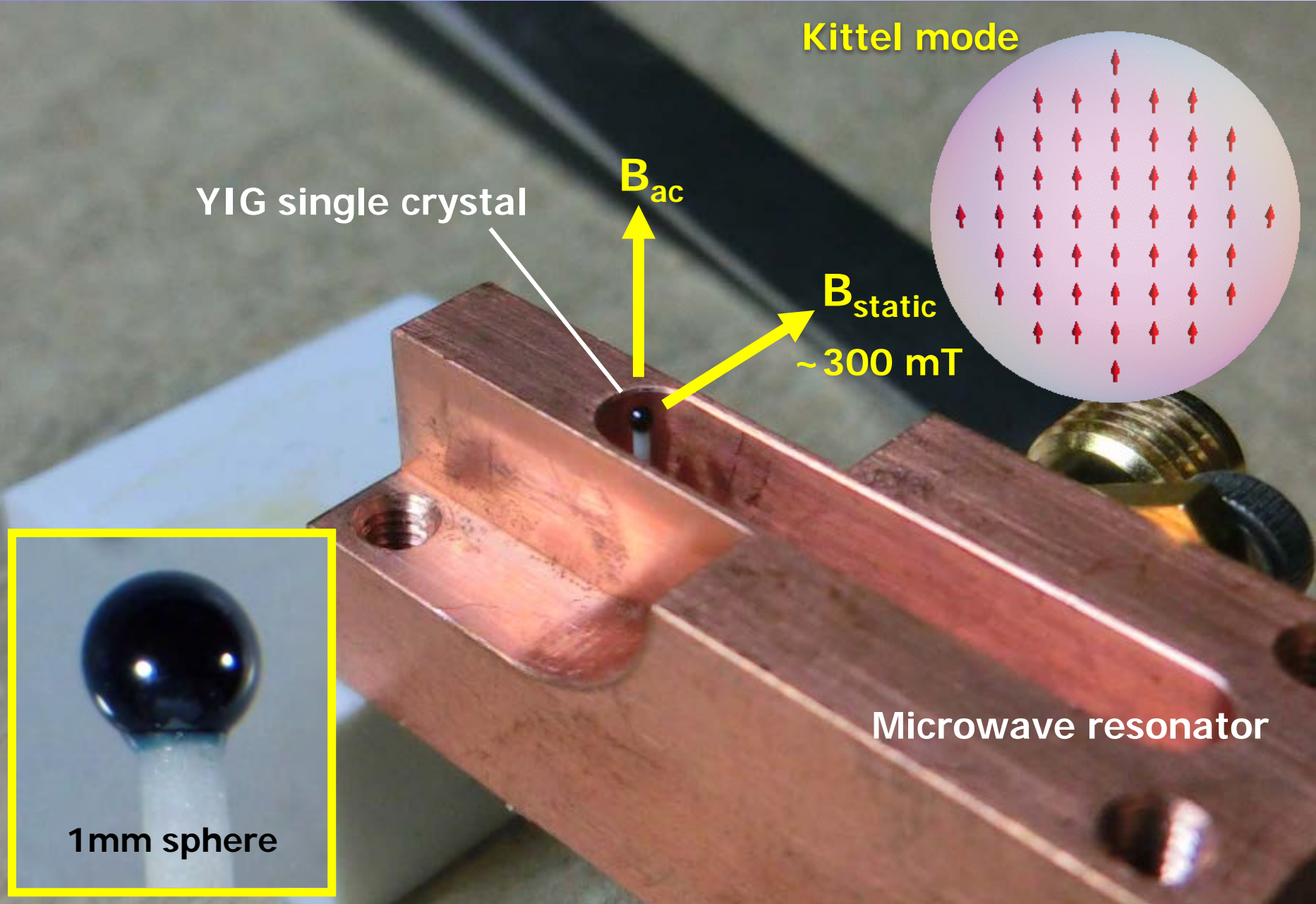
FDK Corporation

Spintronics

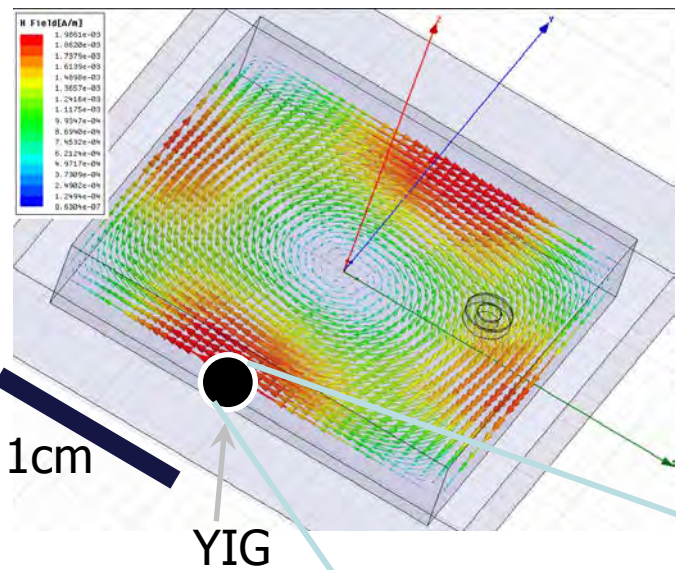


Kajiwara et al.
Nature 2010

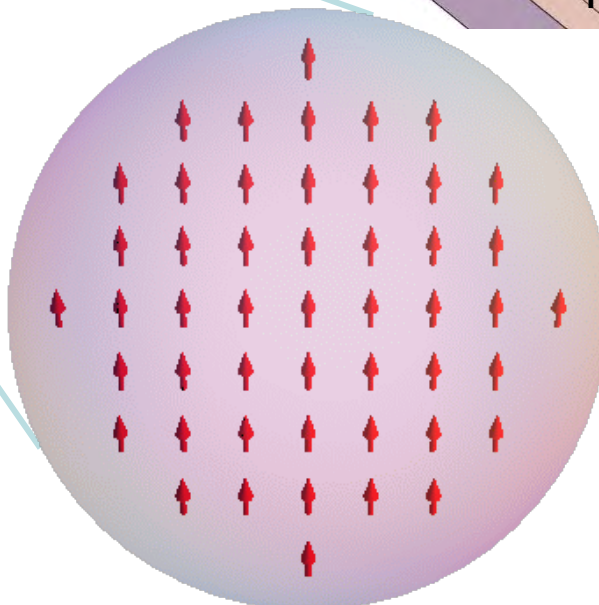
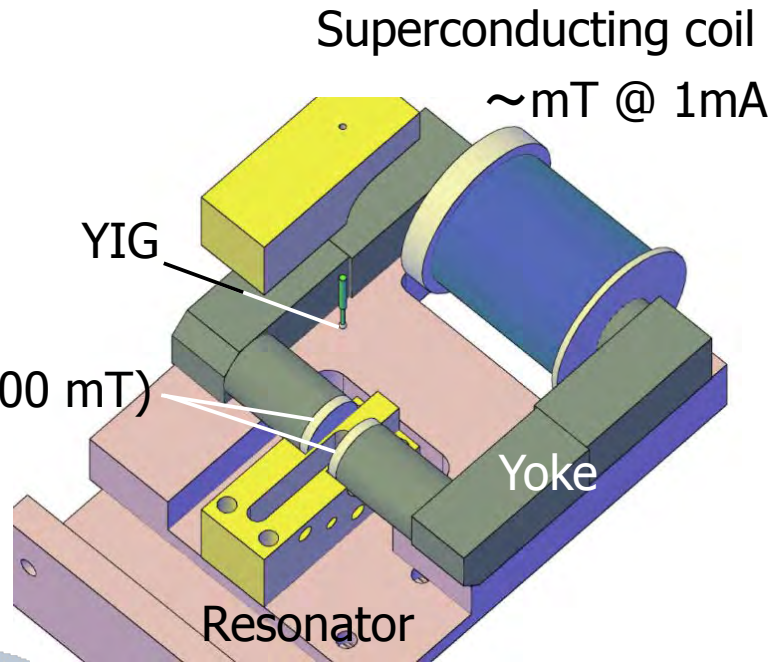
Hybrid with ferromagnet magnons



Experimental setup

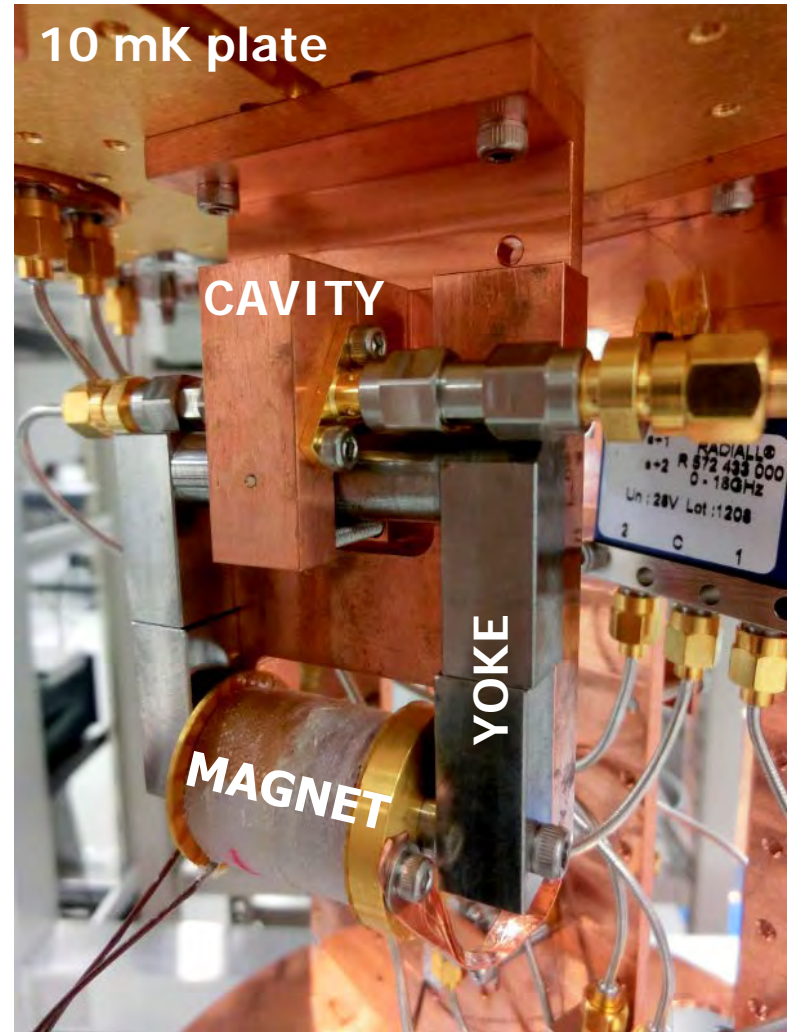
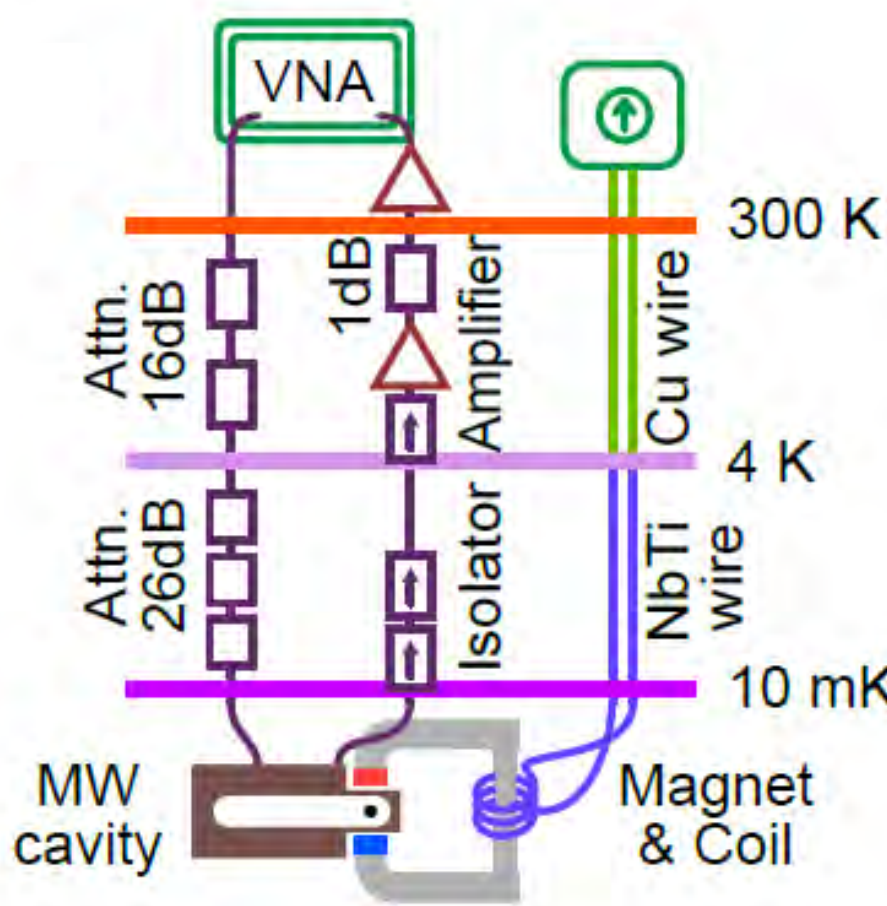


Copper resonator
Rectangular TE₁₀₁ mode



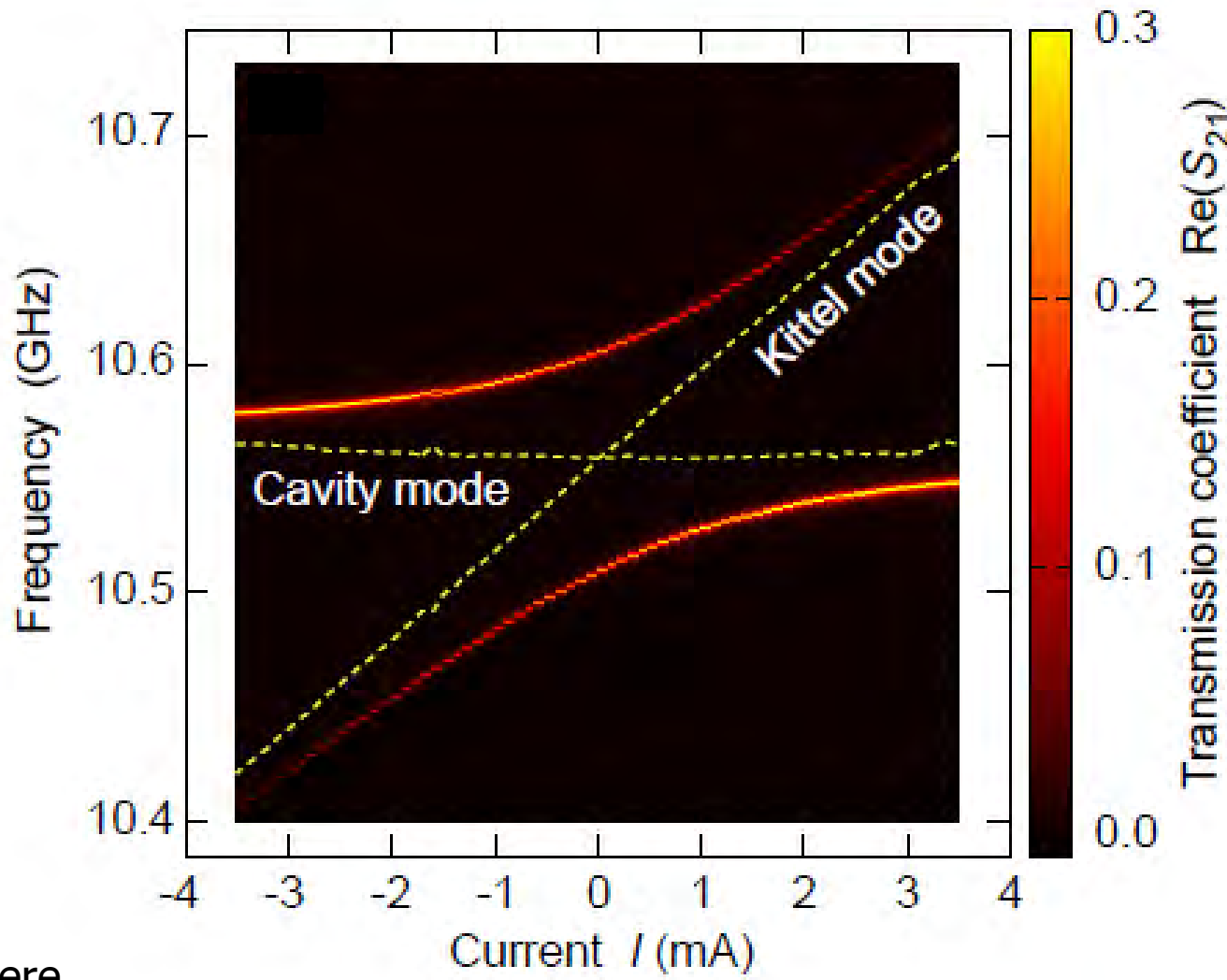
- ▶ Copper resonator
Rectangular TE₁₀₁ mode
- ▶ YIG sphere
Magnetostatic mode
with uniform precession
(Kittel mode)

Experimental setup

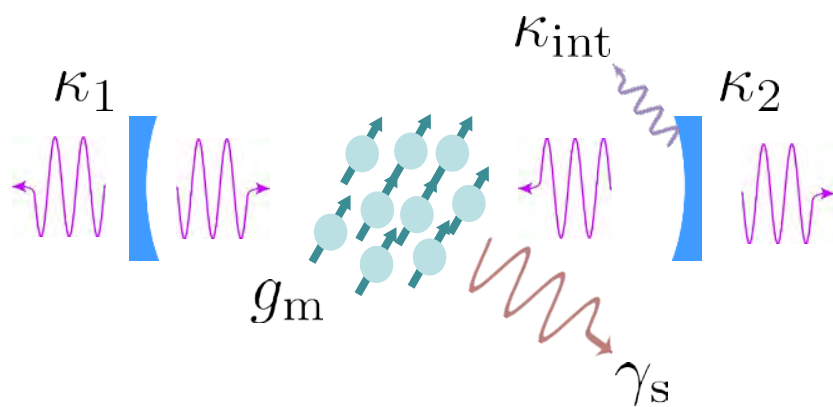


Magnetic-field dependence

Low temperature ~ 10 mK; \square 1 thermal magnon & photon
Microwave power: ~ 0.9 photons in cavity

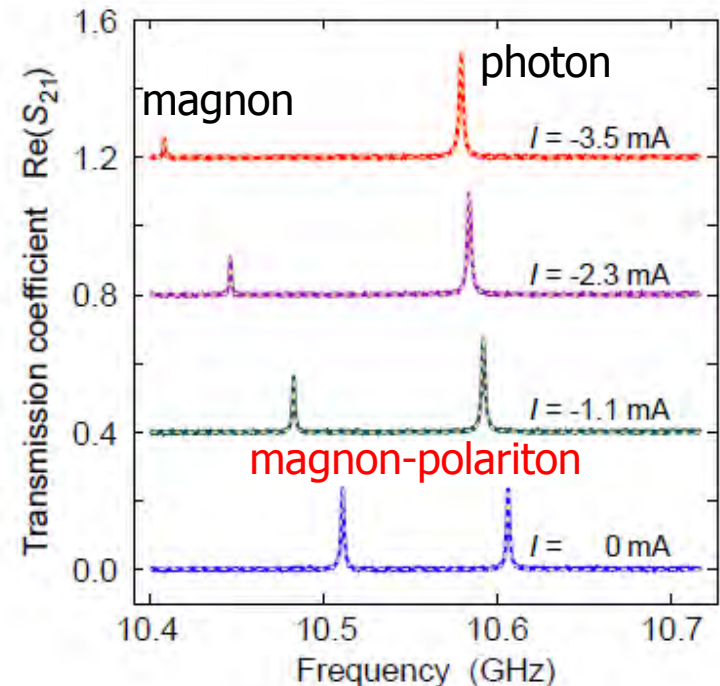


Coupling strength and cooperativity



Strong coupling condition

$$g_m \gg \kappa_{\text{tot}}, \gamma_S$$



	Parameter	Value
Cavity external coupling	$(\kappa_1 + \kappa_2)/2\pi$	1.6 MHz
Cavity intrinsic loss	$\kappa_{\text{int}}/2\pi$	1.1 MHz
Magnon linewidth	$\gamma_S/2\pi$	1.1 MHz
Magnon-photon coupling	$g_m/2\pi$	47 MHz
Cooperativity	$4g_m^2/\gamma_S(\kappa_c + \kappa_{\text{int}})$	3.0×10^3

Sphere-size dependence of coupling strength

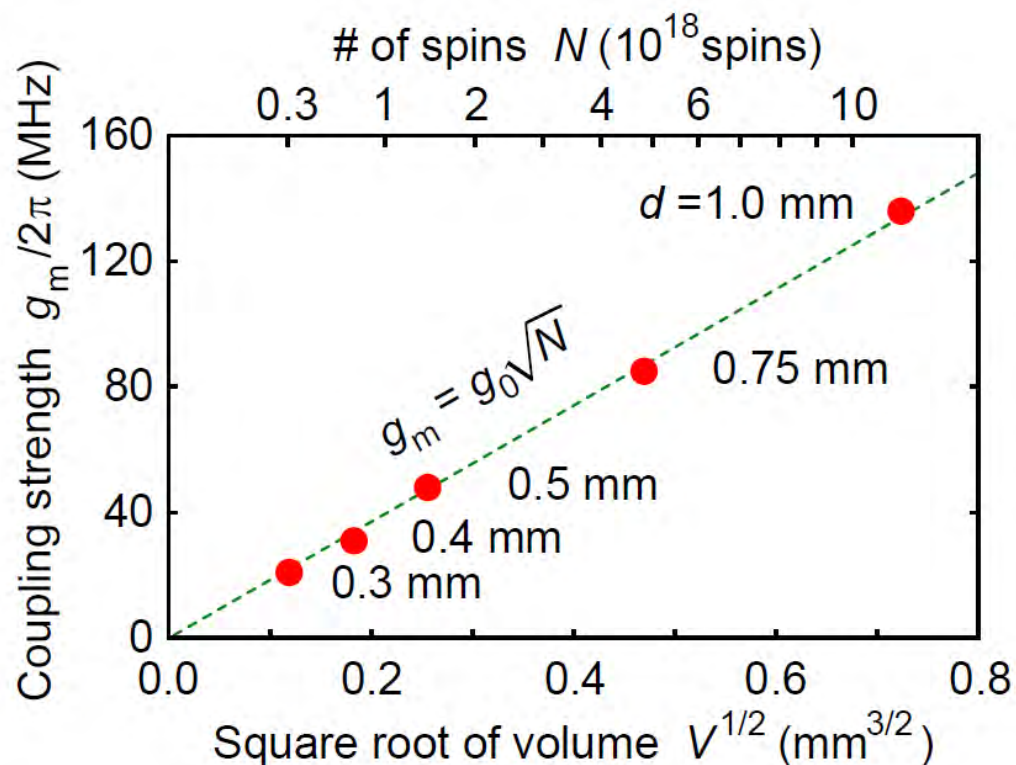
$$g_m = g_0 \sqrt{N}$$

$$d = 1 \text{ mm}$$

$$N = 1.1 \times 10^{19} \text{ spins}$$

→ $g_0/2\pi = 39 \text{ mHz}$

Coupling strength per spin

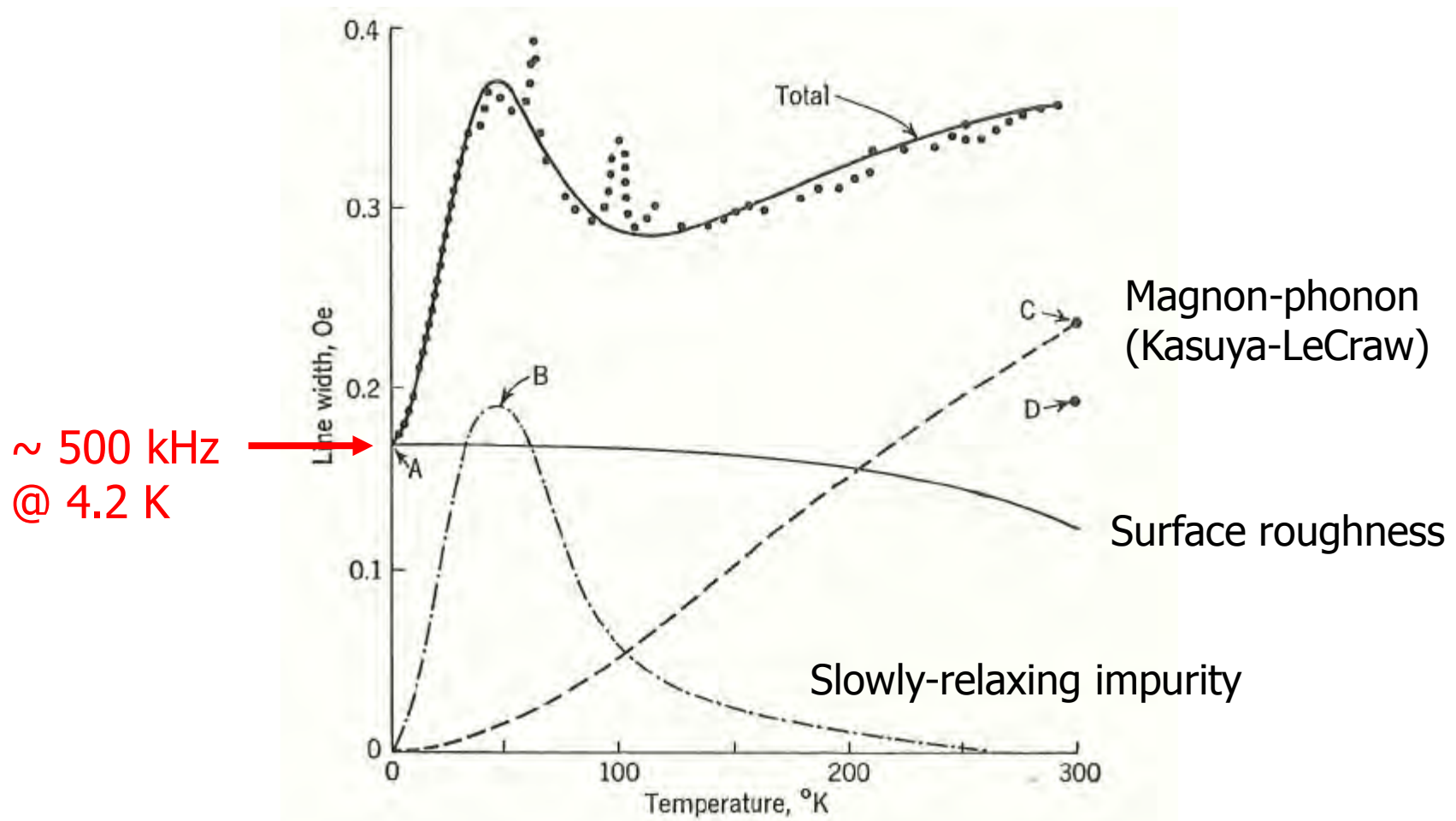


Estimation from vacuum fluctuation amplitude

$$g_0/2\pi = g\mu_B B_{\text{vac}}/2\pi\hbar \sim 38 \text{ mHz}$$

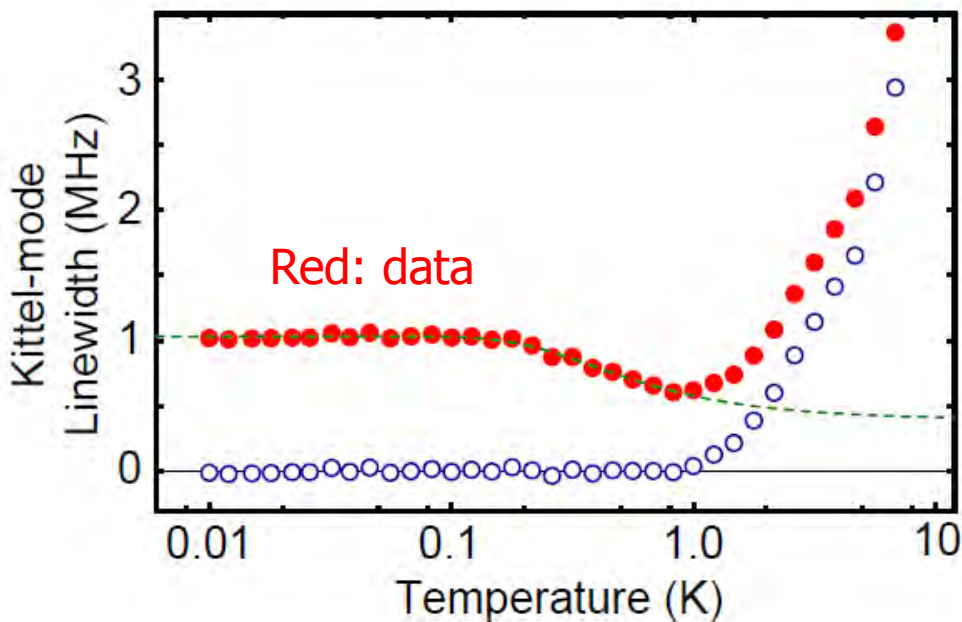
$$B_{\text{vac}} = \sqrt{\frac{\mu_0 \hbar \omega_r}{2V_r}} \sim 10 \text{ nG}$$

Magnon linewidth vs. temperature



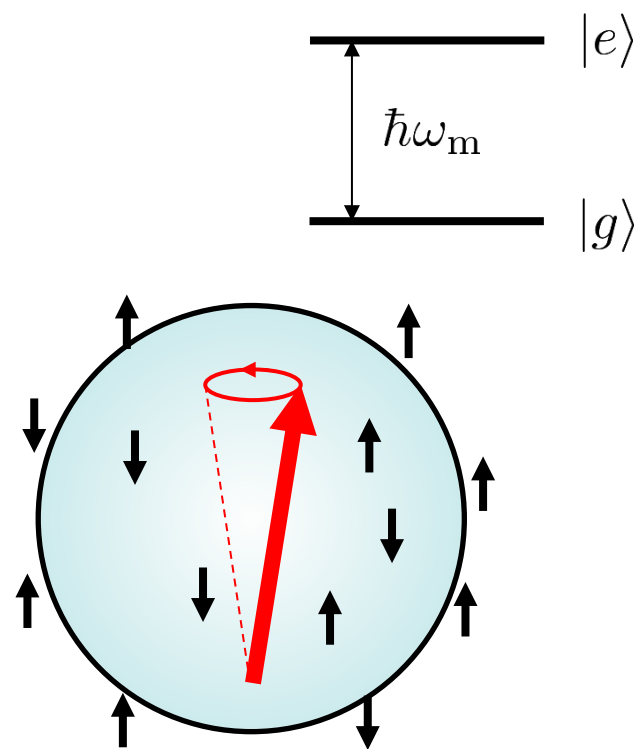
M. Sparks, Ferromagnetic-Relaxation Theory (1964);
Data: E. G. Spencer et. al. Phys. Rev. Lett. 3, 32 (1959).

Magnon linewidth vs. temperature



$$\Delta\omega \propto \tanh\left(\frac{\hbar\omega_m}{2k_B T}\right)$$

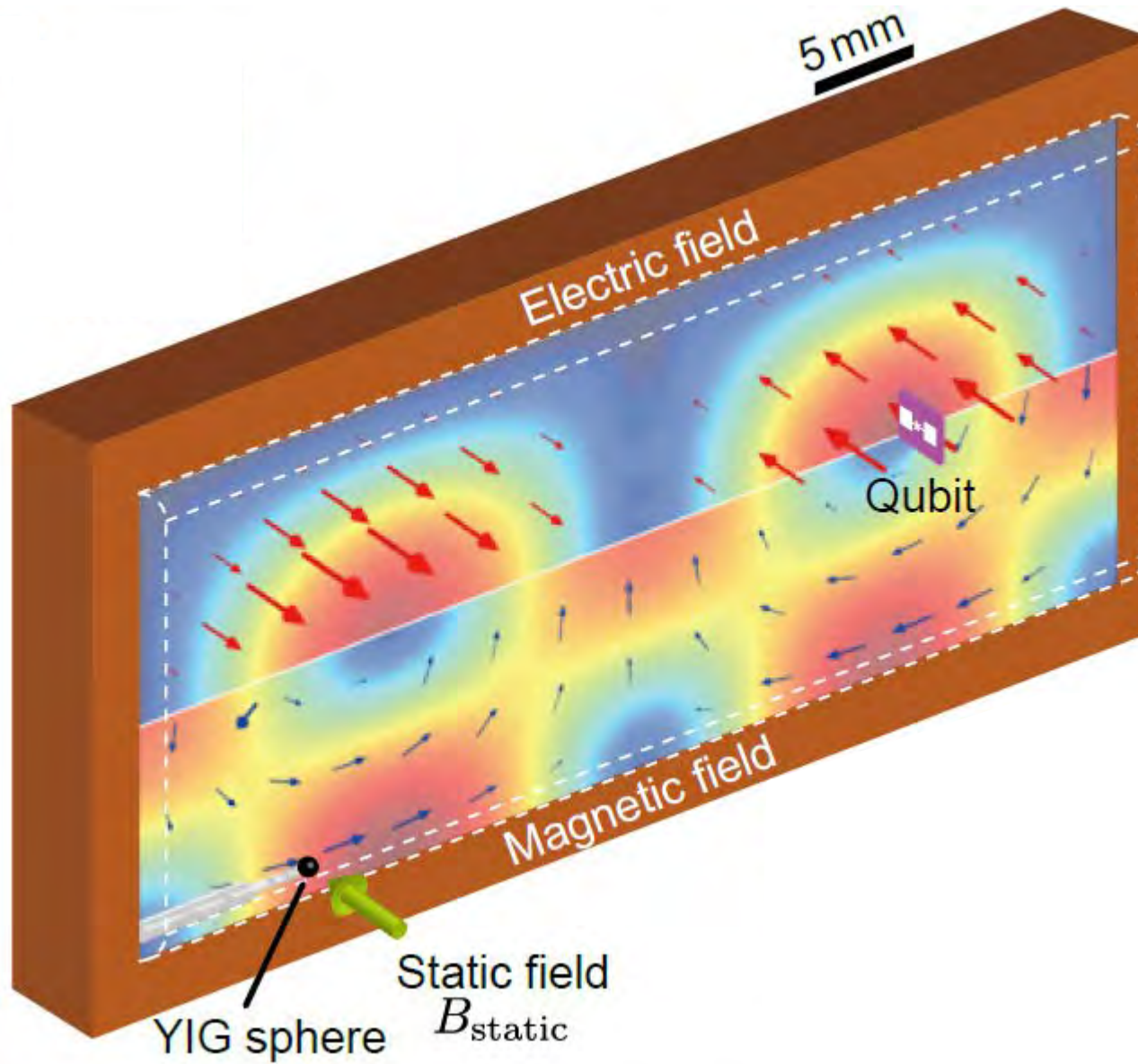
Coupling to ensemble of two-level systems



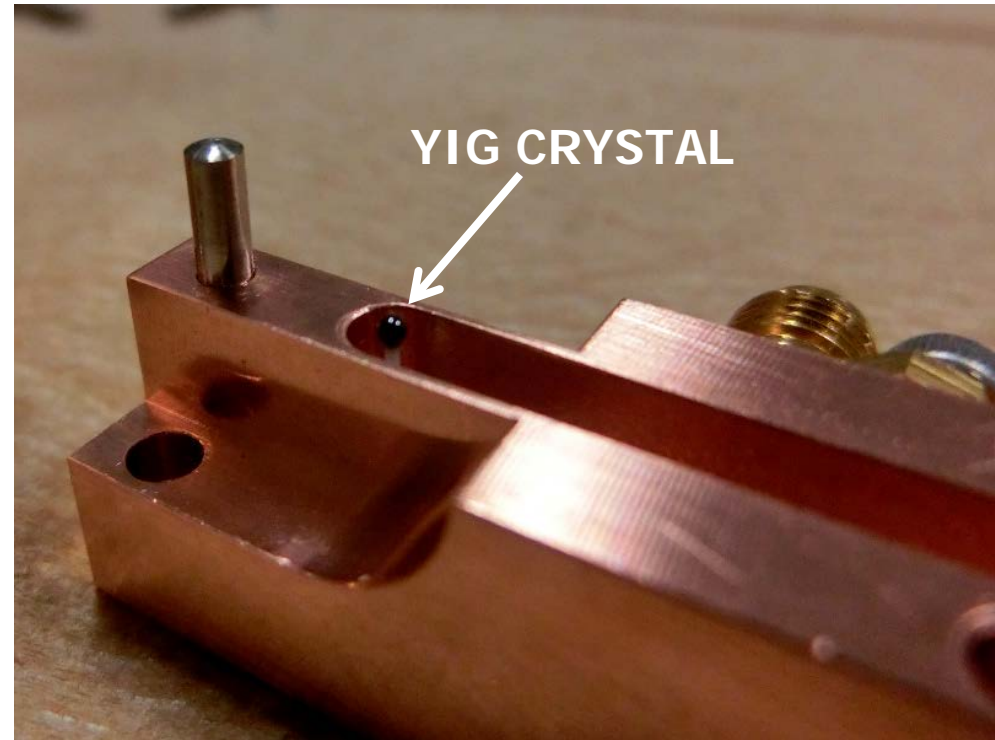
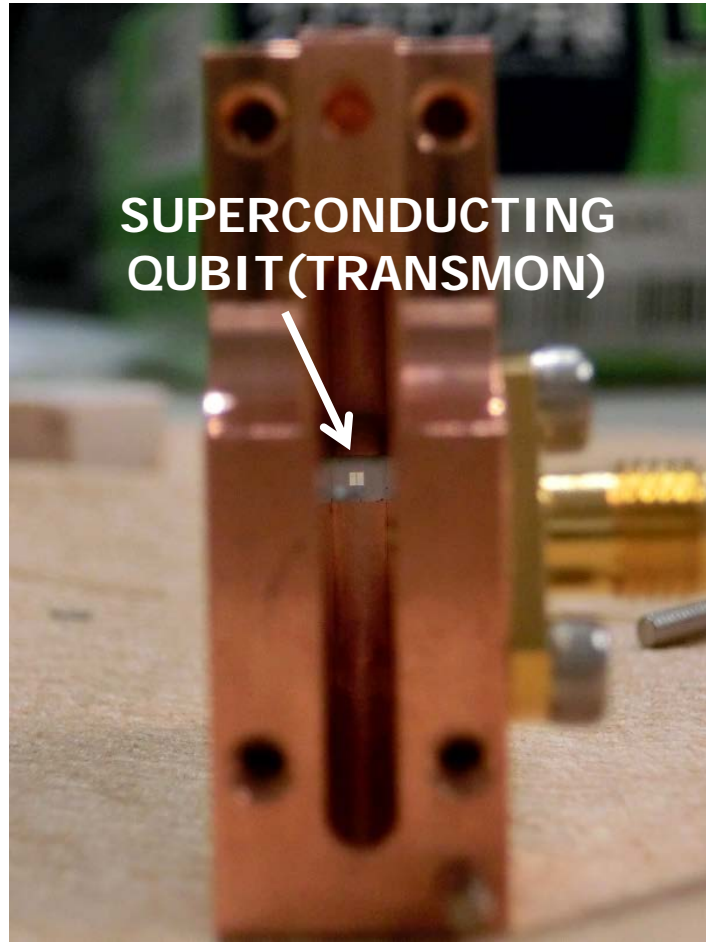
cf. superconducting resonator, Martinis 2005
glass physics, Hunklinger ~1980

Theory: J. H. Van Vleck, J. Appl. Phys. 35, 882 (1964).

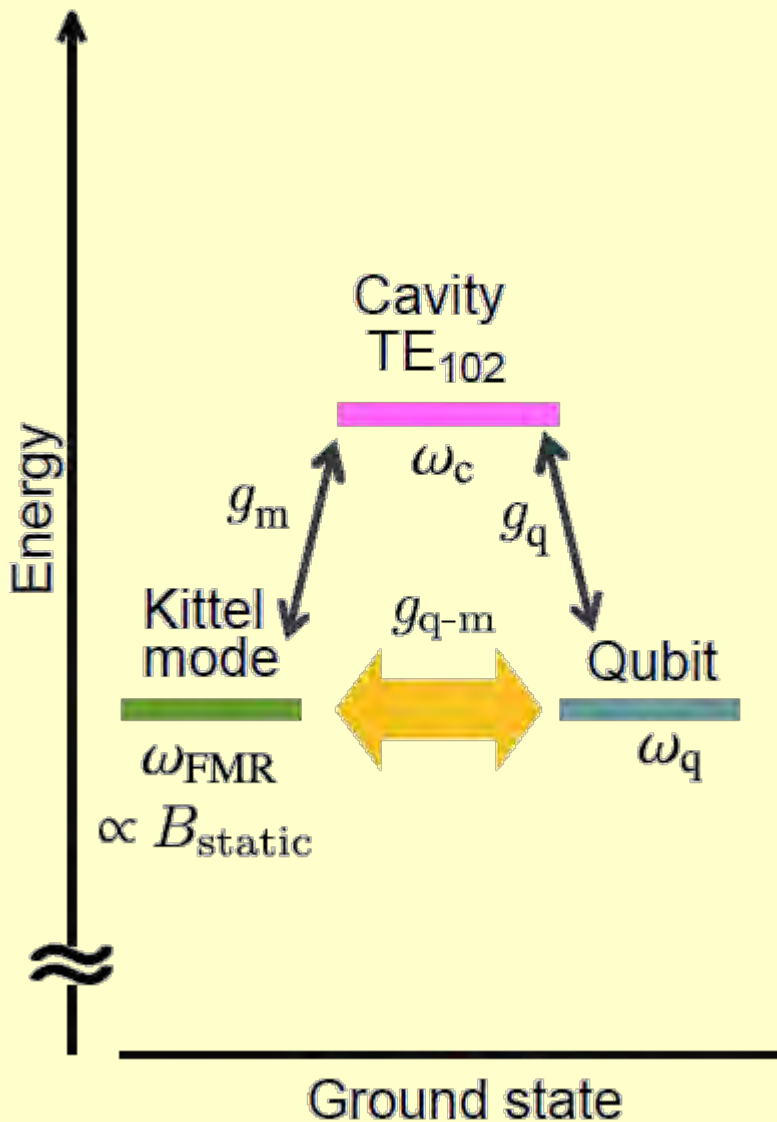
Coupling with a superconducting qubit



Inside the cavity



Qubit-magnon coupling

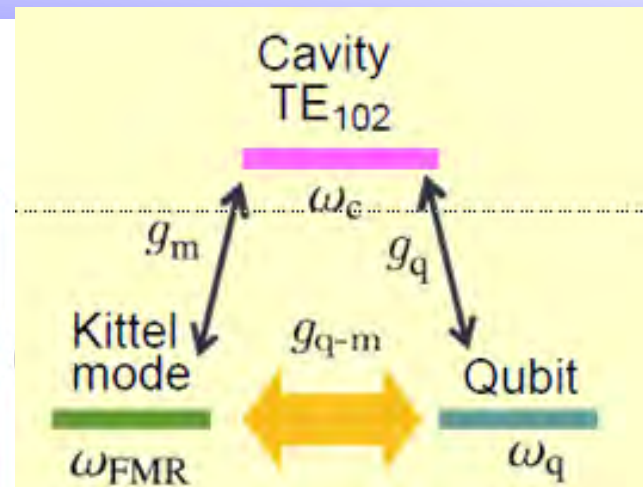
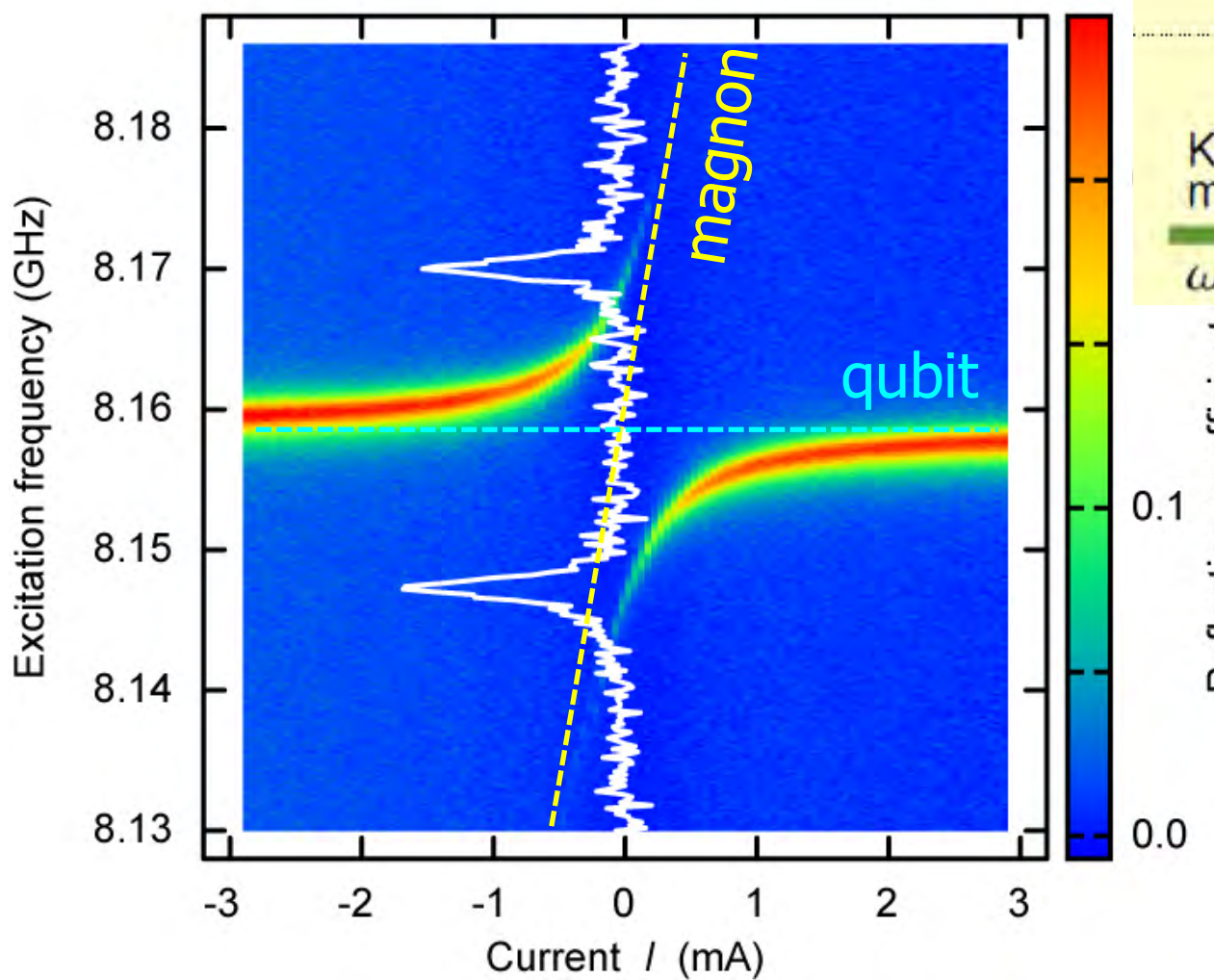


Qubit-magnon coupling
mediated by virtual photon excitation
in cavity

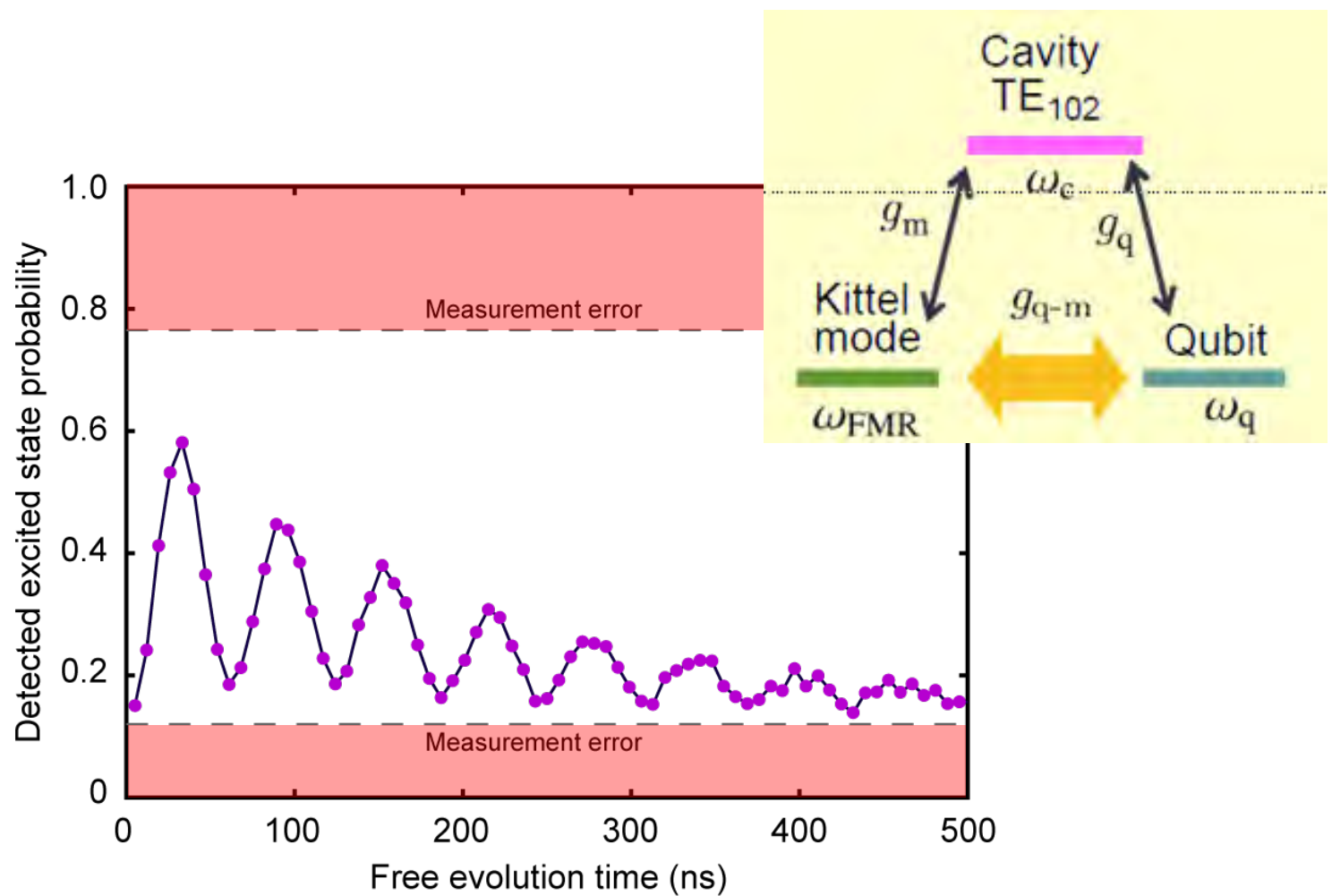
$$\hat{\mathcal{H}}_{q\text{-}m}/\hbar \sim g_{q\text{-}m} (\hat{a}_m^\dagger \sigma_- + \hat{a}_m \sigma_+)$$

$$g_{q\text{-}m}/\hbar = \frac{g_q g_m}{\omega_c - \omega_q}$$
$$\sim 10\text{-}50 \text{ MHz}$$

Vacuum Rabi splitting

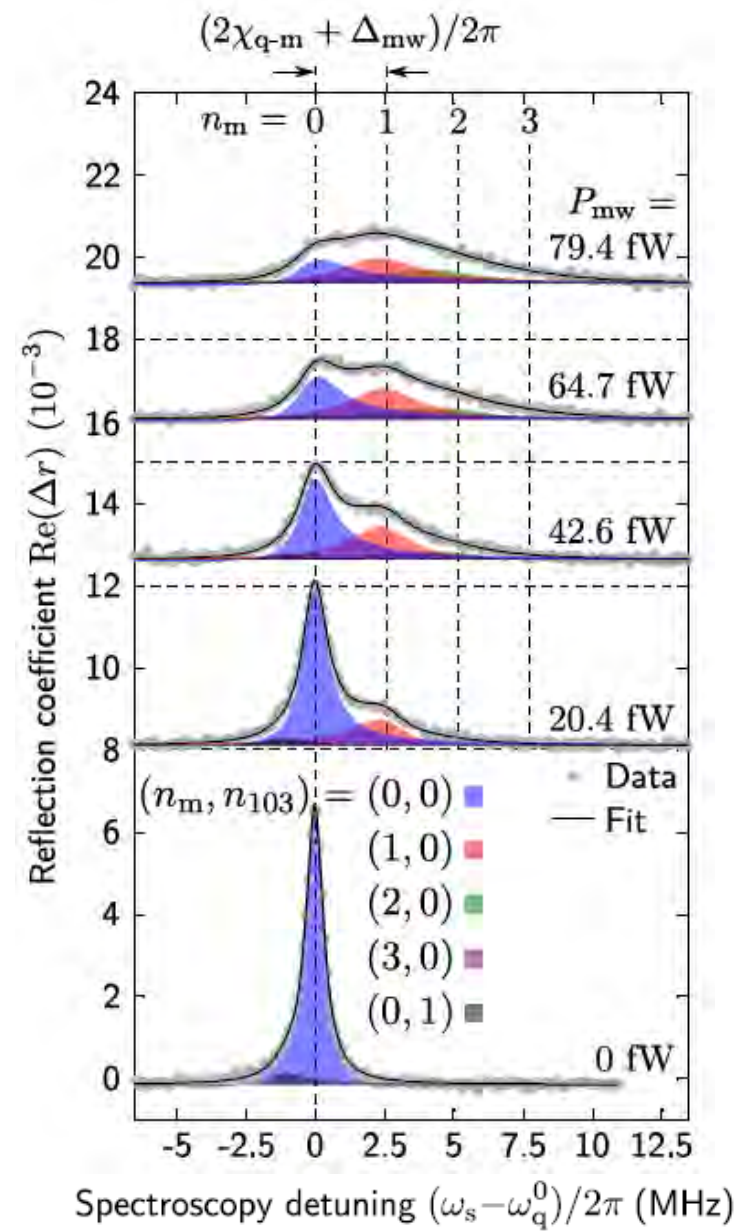
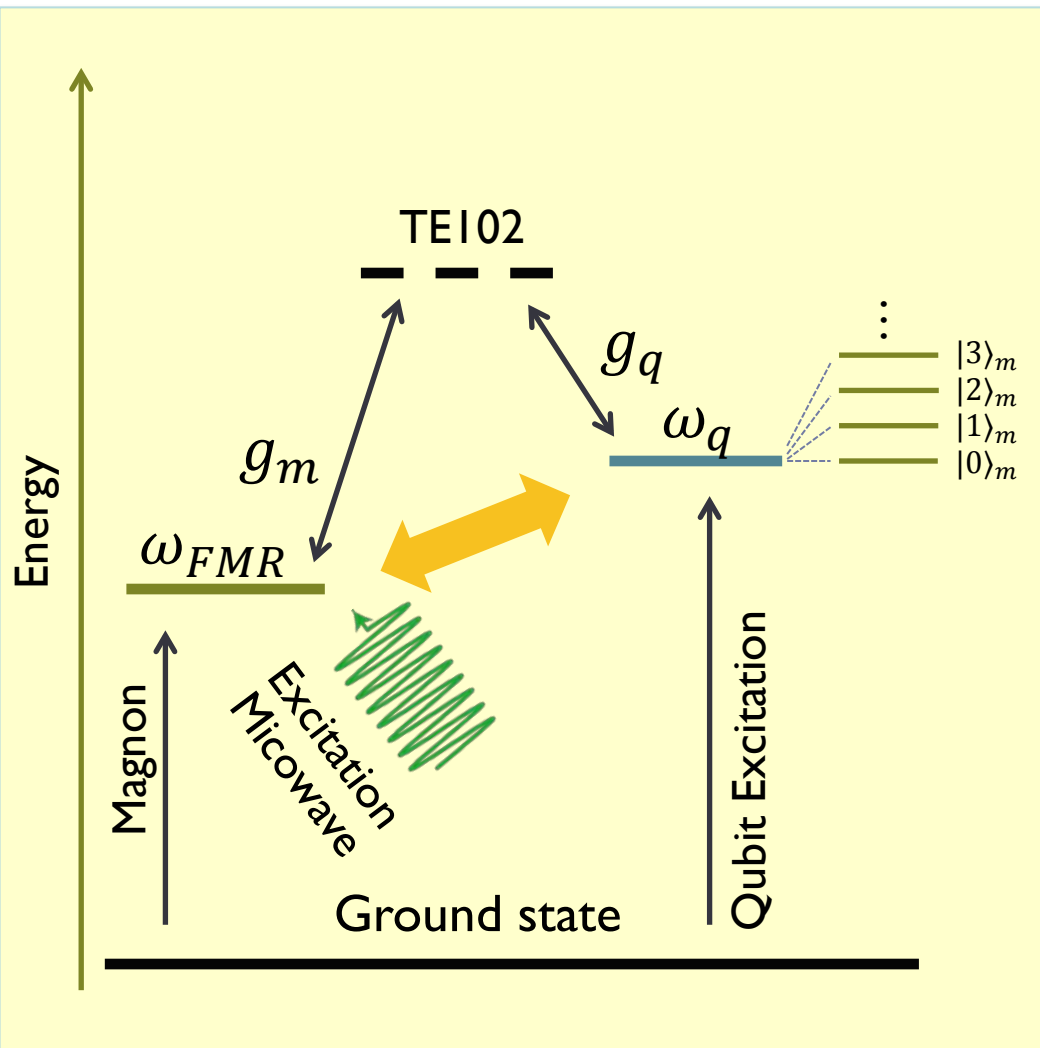


Vacuum Rabi oscillations



Magnon-number-resolving spectroscopy

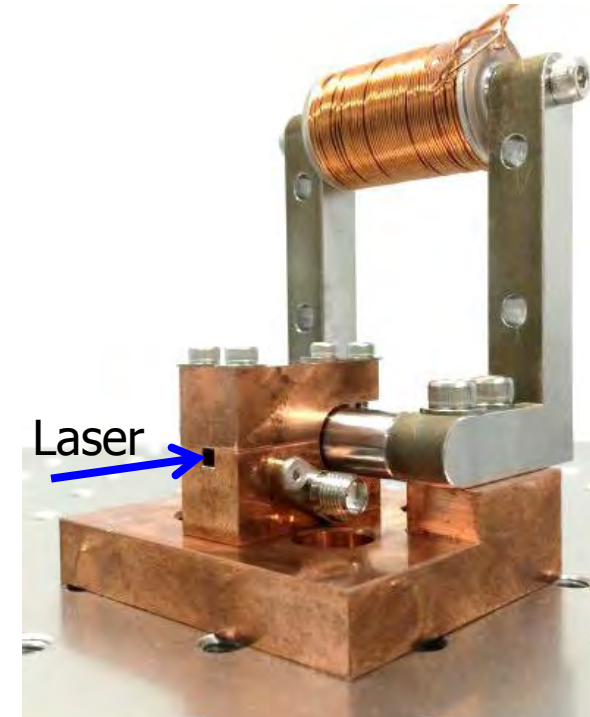
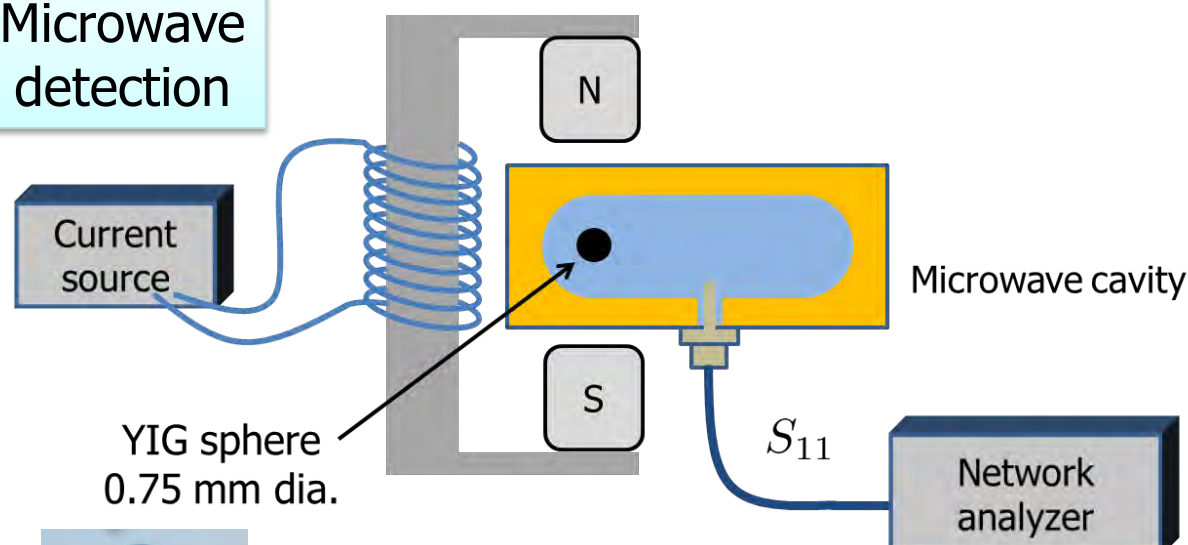
D. Lachance-Quirion et al.
unpublished



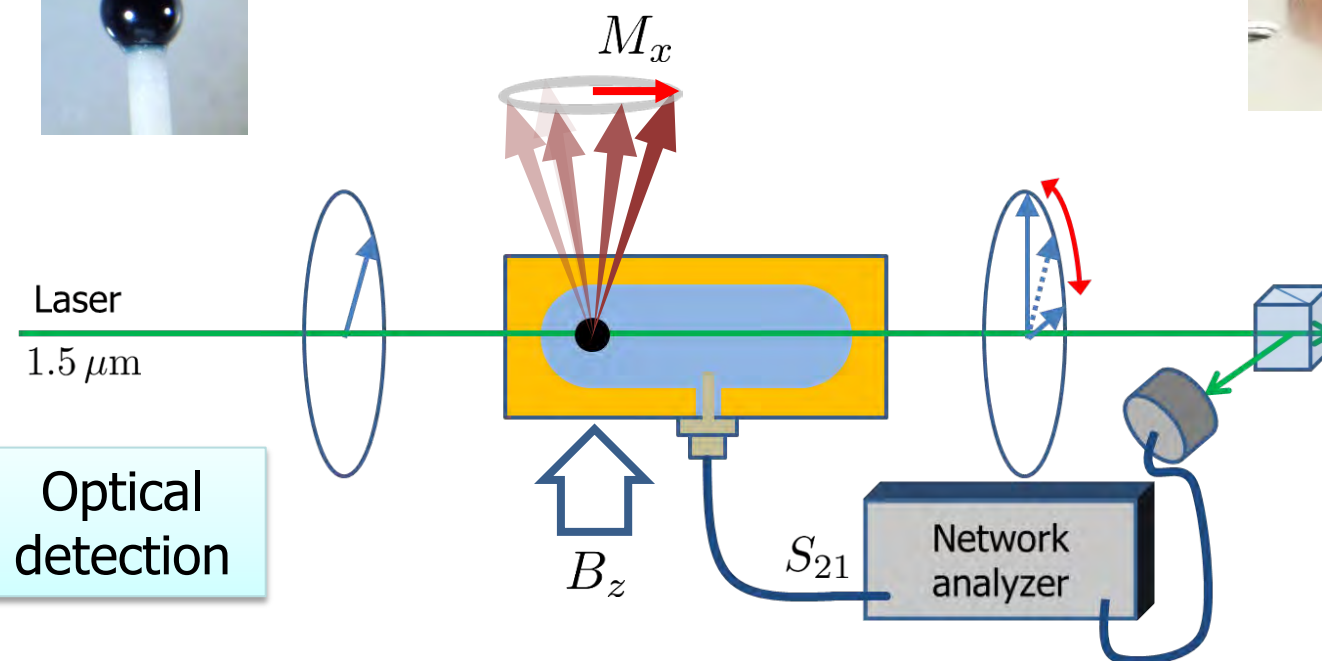
(Quantum) optomagnonics

Optical detection of magnon excitations

Microwave
detection



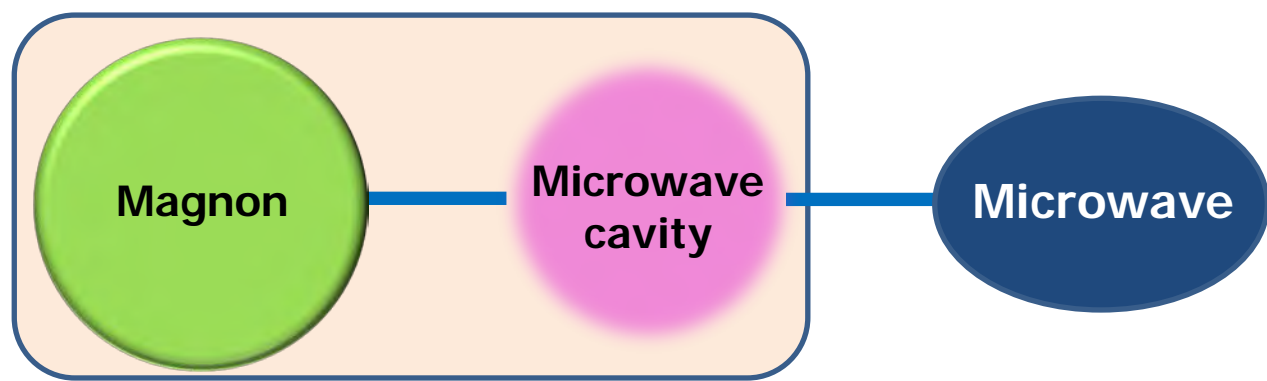
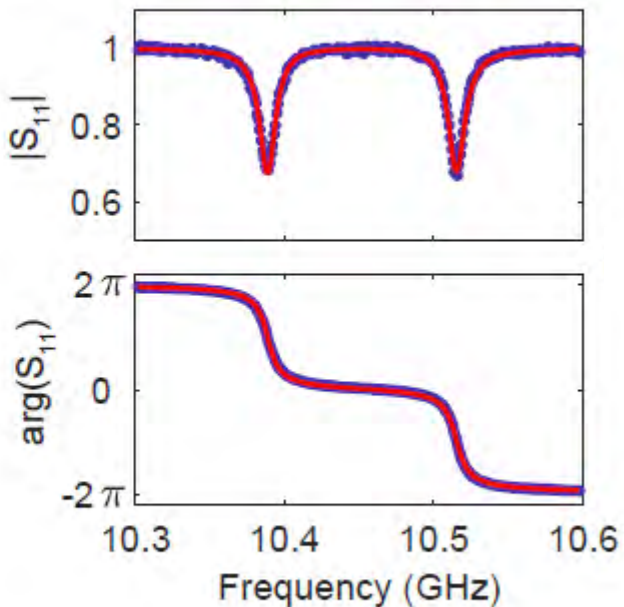
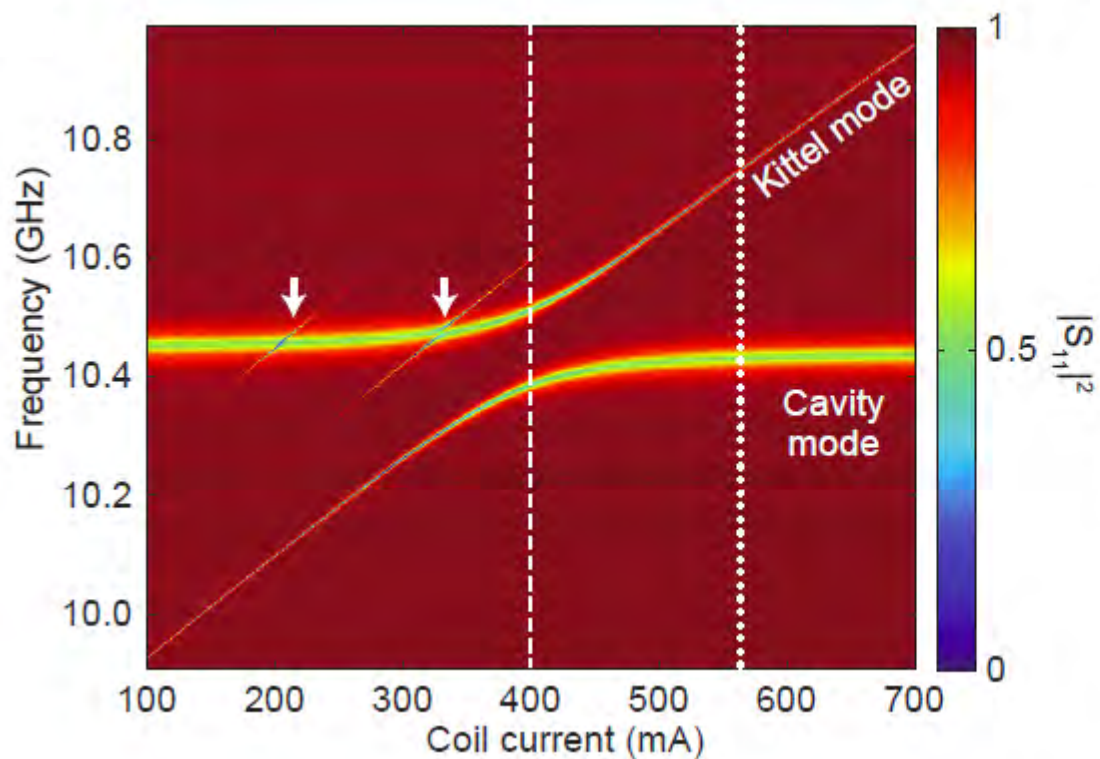
Optical
detection



R. Hisatomi et al.
arXiv:1601.03908;
to appear in PRA

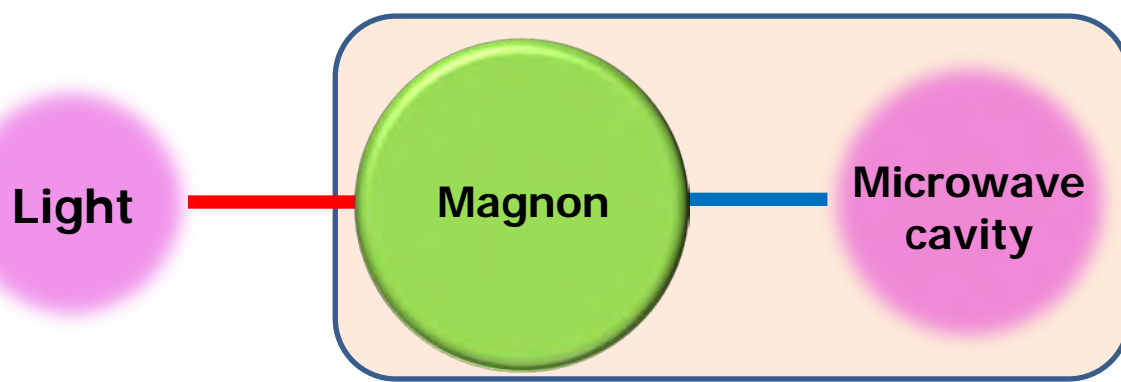
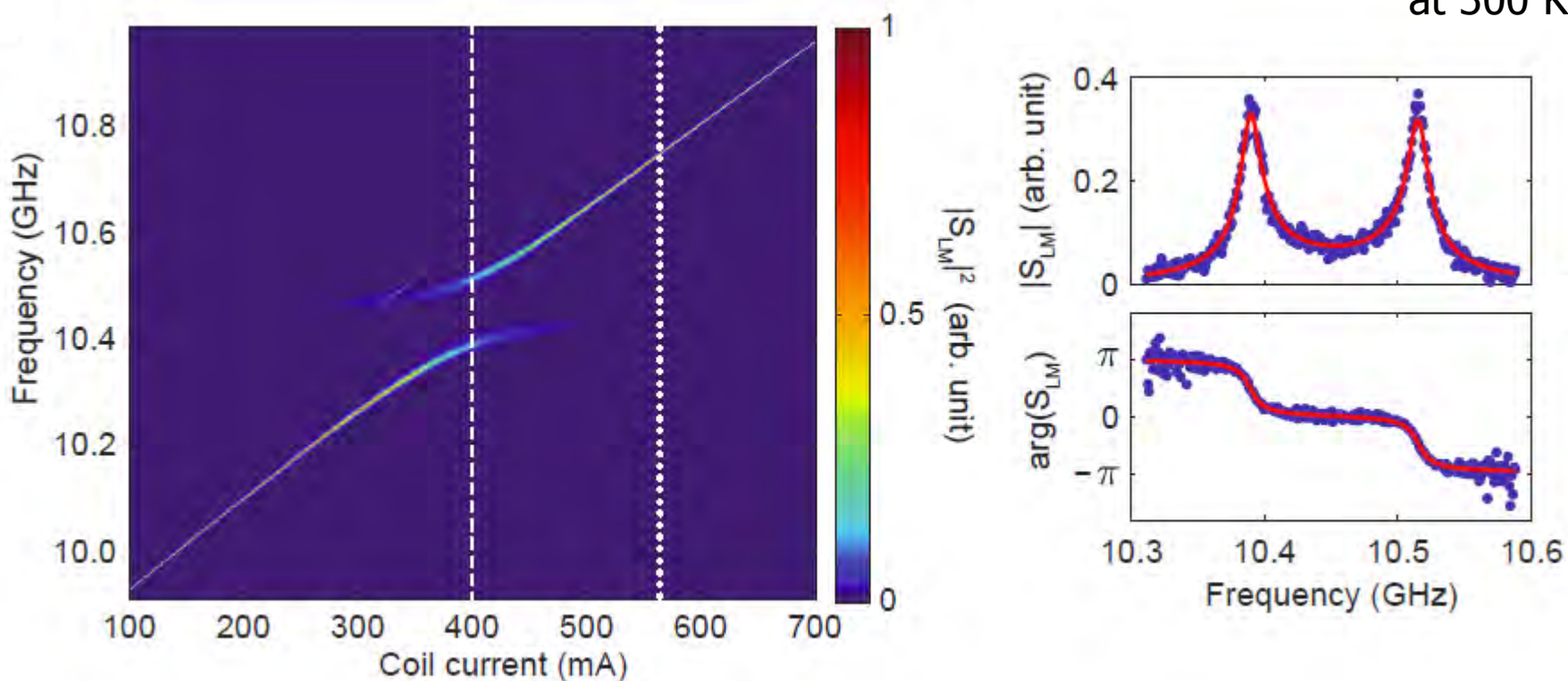
Optical detection of magnon excitations

at 300 K



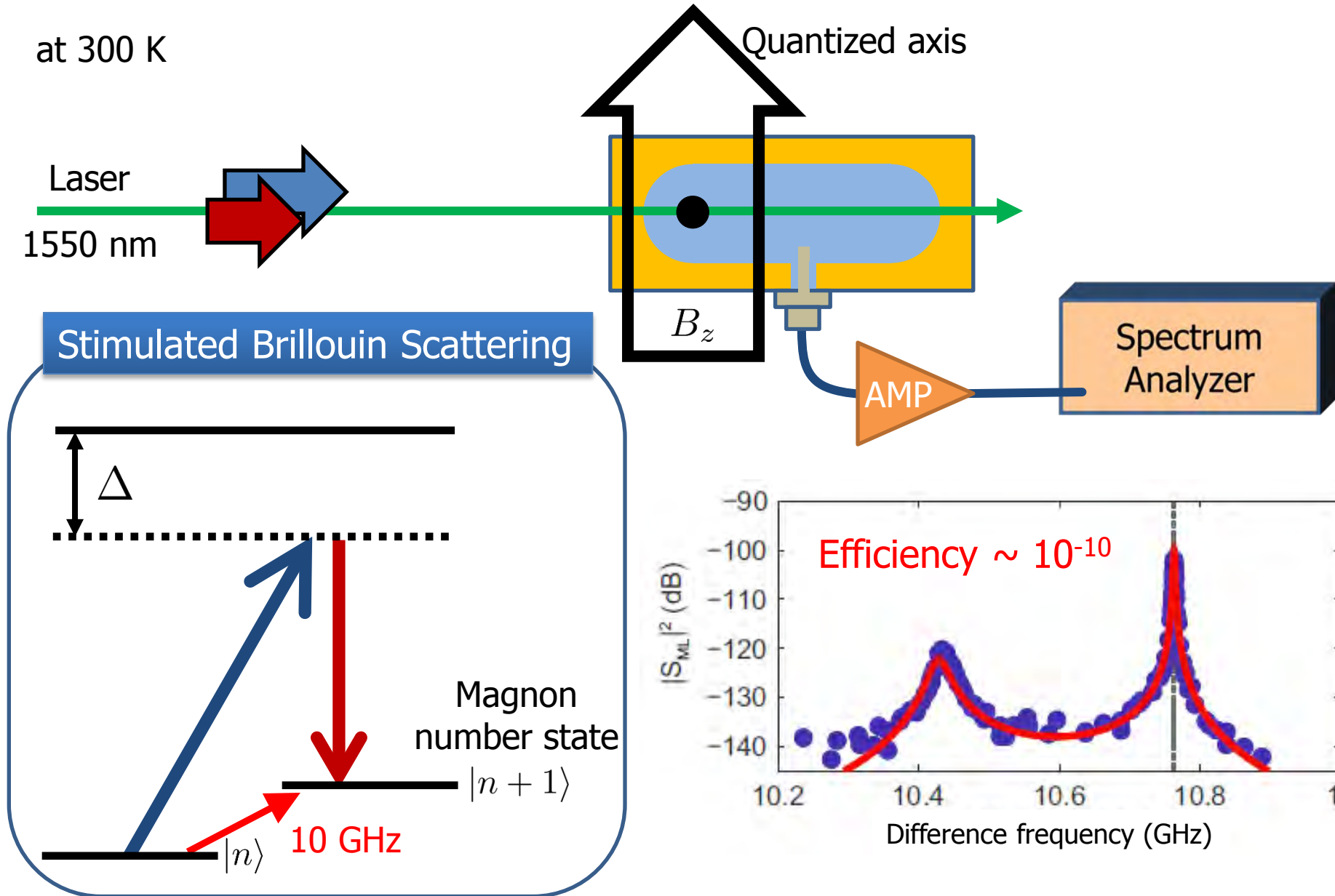
Optical detection of magnon excitations

at 300 K



Coherent microwave generation via magnon Brillouin scattering

at 300 K



Cavity optomagnonics

See also

J. A. Haigh et al. PRA 92, 063845 (Cambridge)
X. Zhang et al. arXiv:1510.03545 (Yale)

Coupling to whispering gallery mode

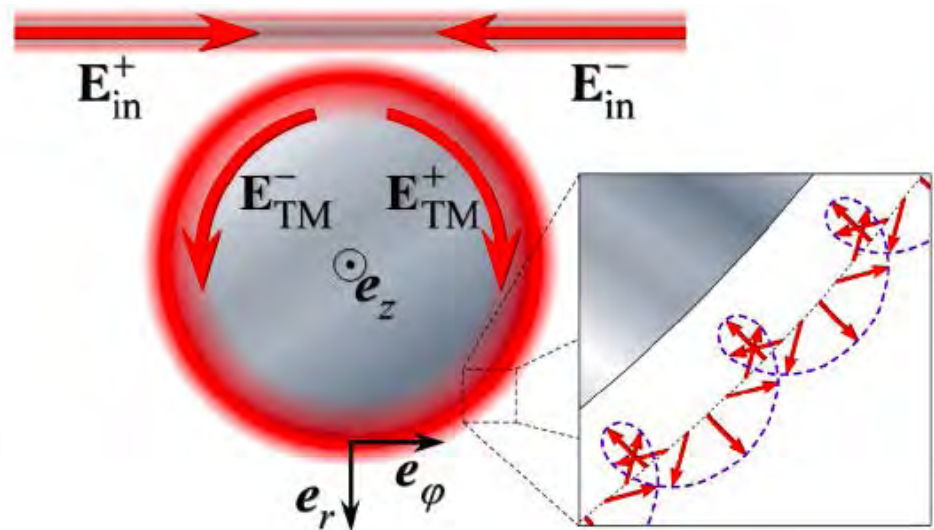
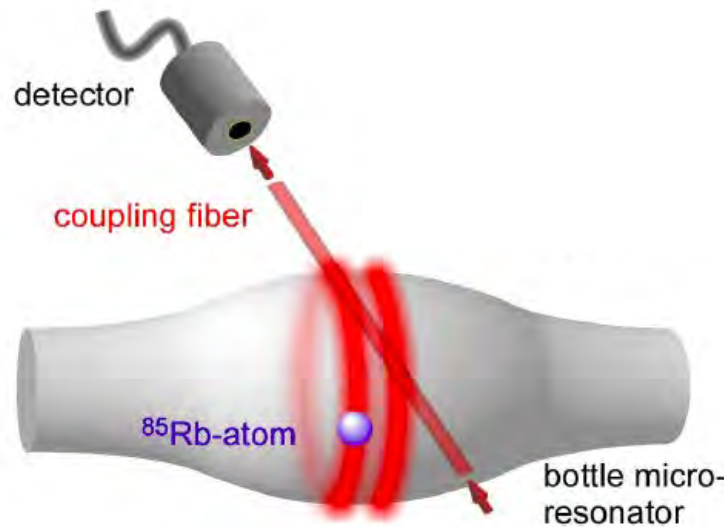
Loop Coil

YIG
(750 μ m)

Nanofiber

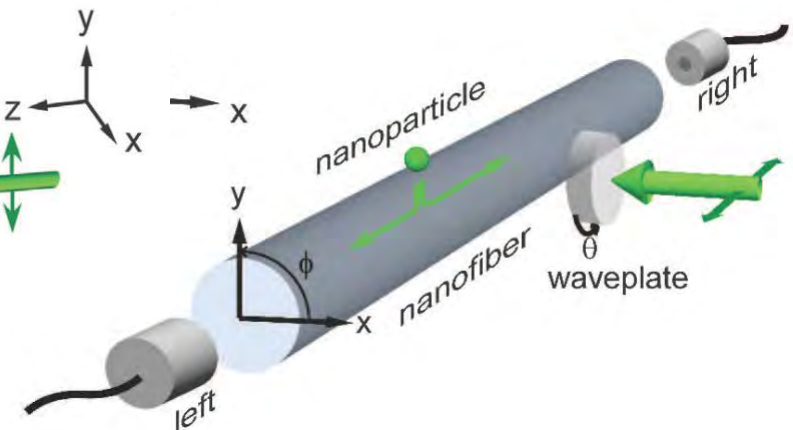
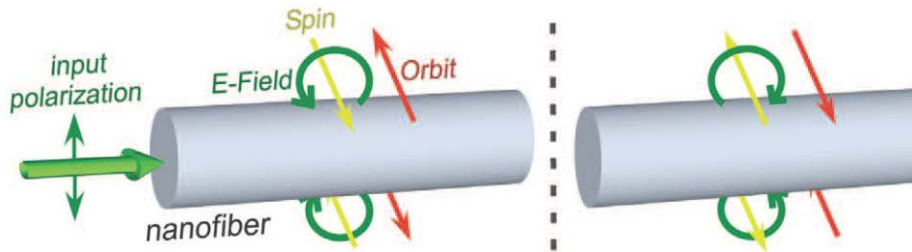
Photonic chiral modes

Chirality in WGM



Junge et al. PRL 110, 213604 (2013) TUWien

Chiral nanophotonic waveguide

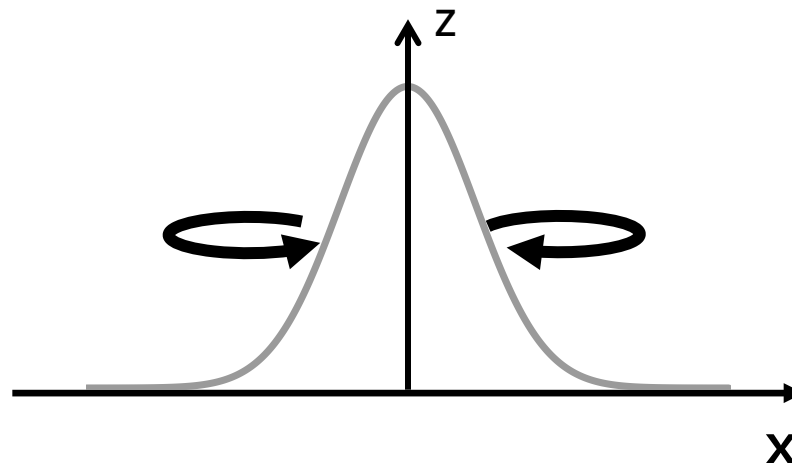


Petersen et al. Science 346, 67 (2014) TUWien

Beyond paraxial approximation

$$\operatorname{div}E = \partial_{\perp}E_{\perp} + \partial_zE_z = 0$$

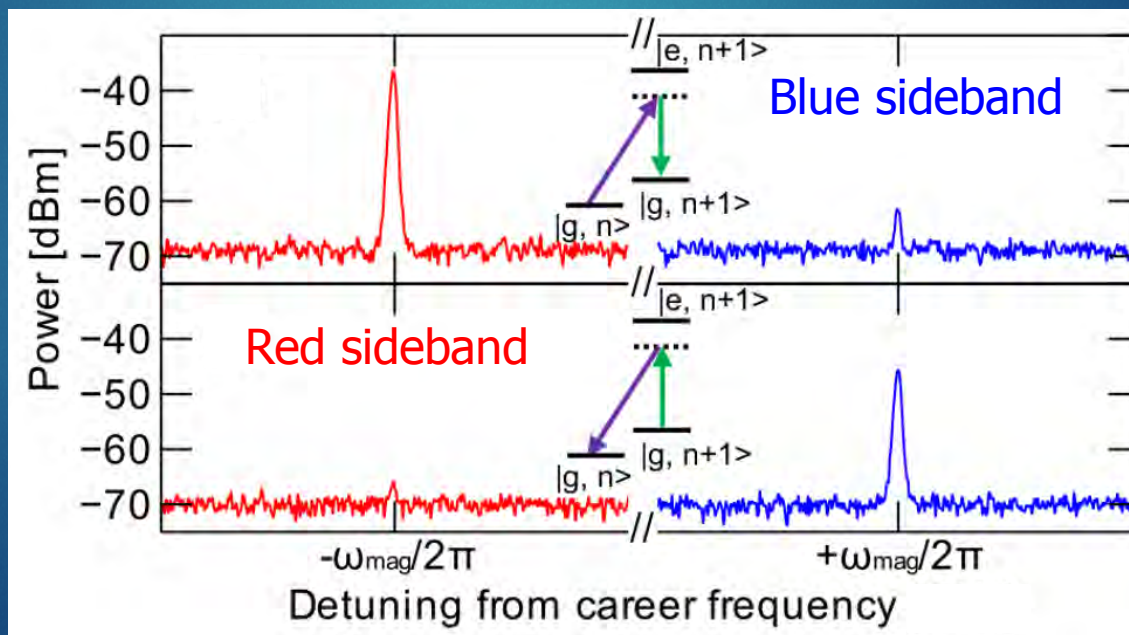
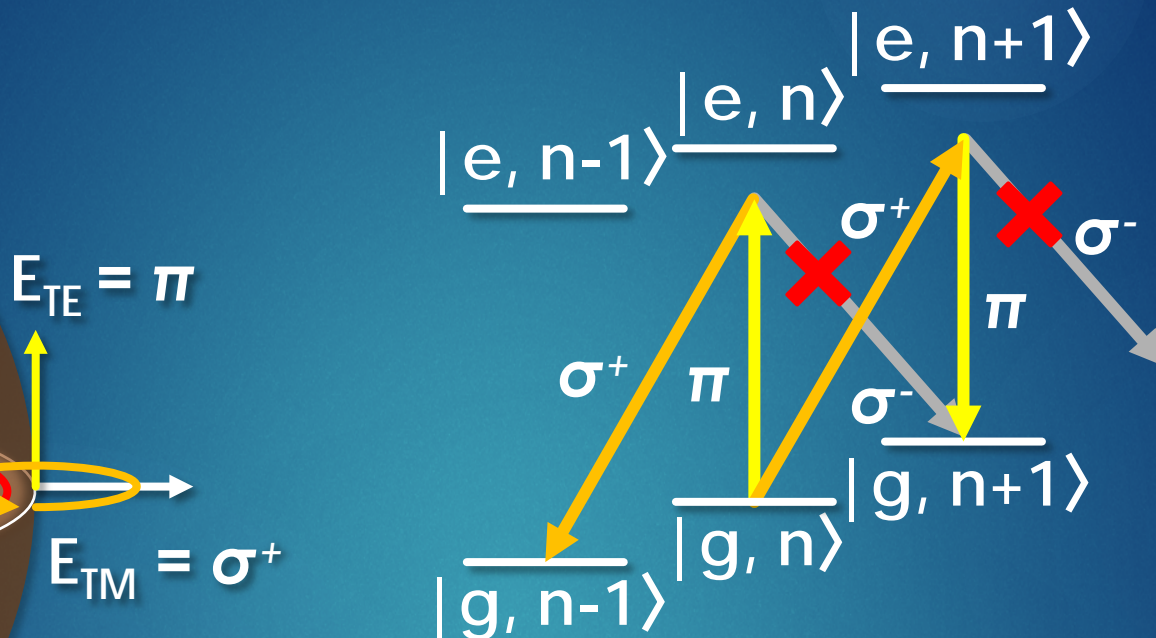
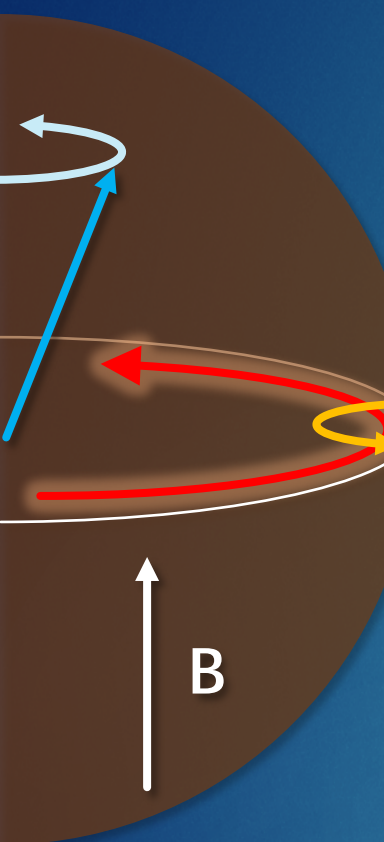
$$\partial_{\perp}E_{\perp} = -ikE_z \quad =0 \text{ for plane wave}$$



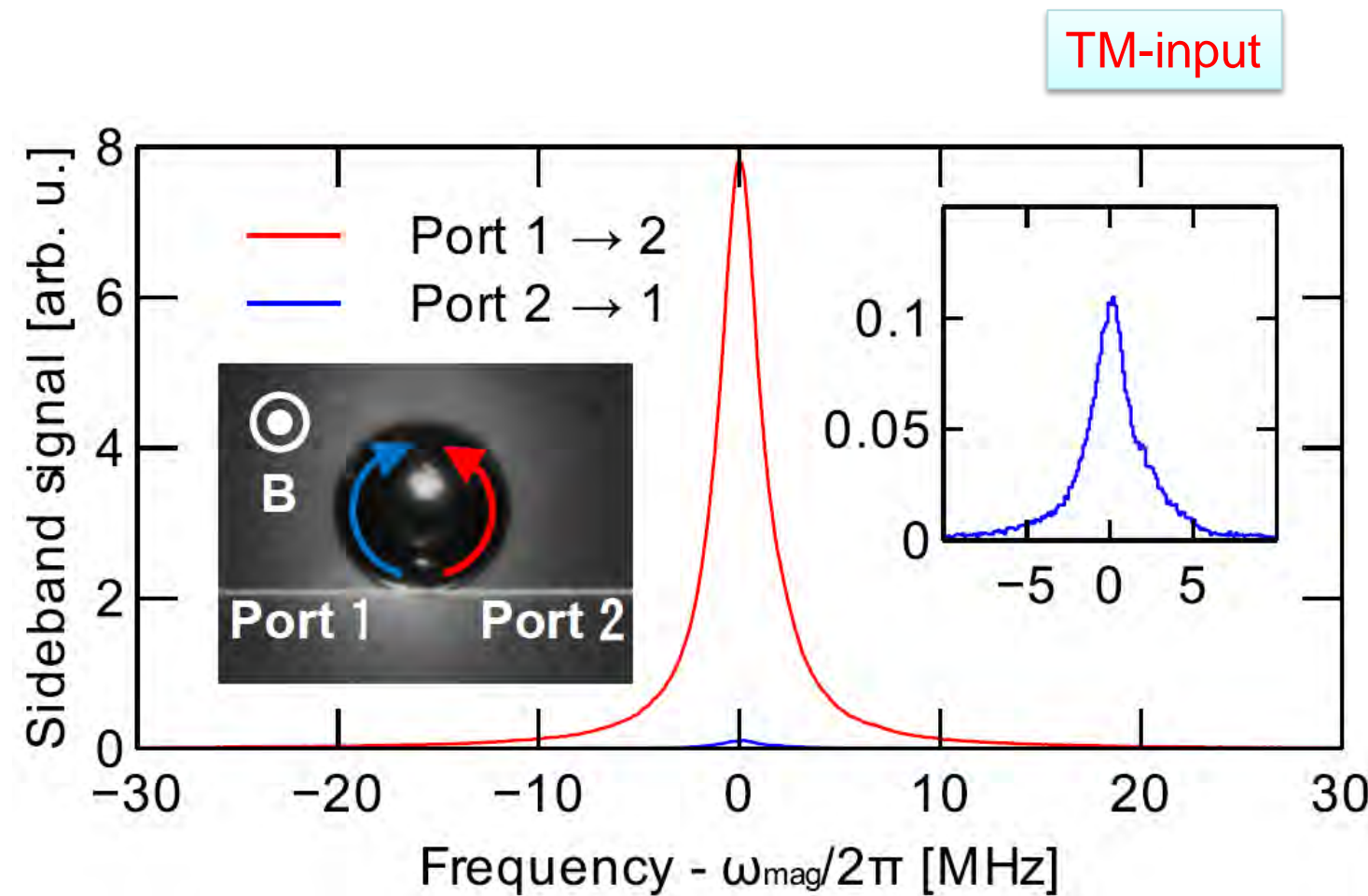
Spin–orbit interactions of light

Review: K. Y. Bliokh et al. Nat. Photo. 9, 796 (2015)

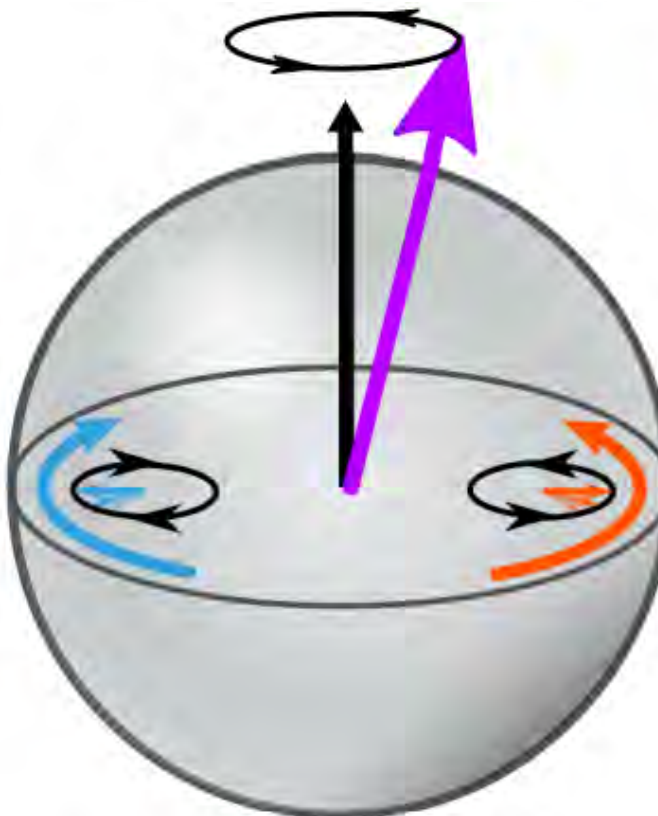
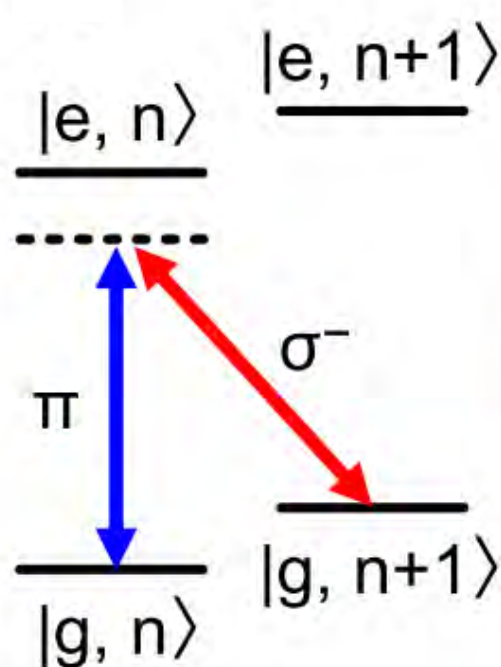
Angular momentum selection rule



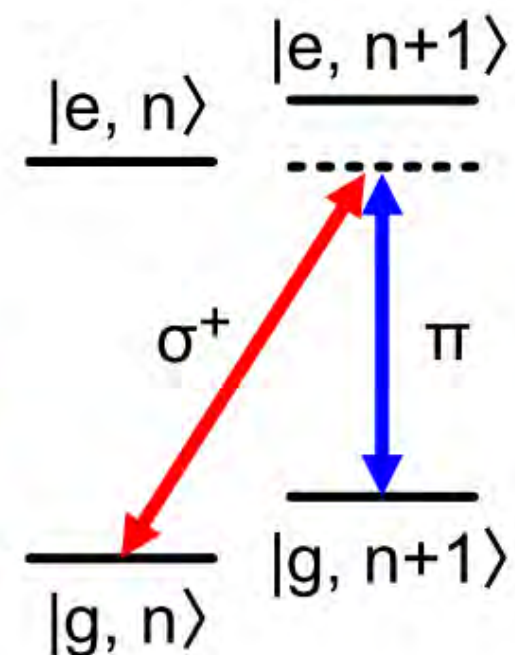
Non-reciprocal sideband generation



Non-reciprocal sideband generation



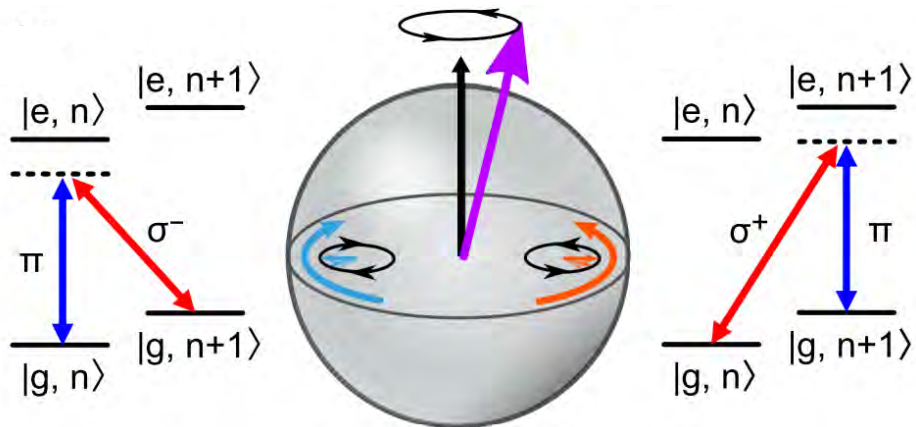
TM-input



$$\omega_{TM} < \omega_{TE}$$

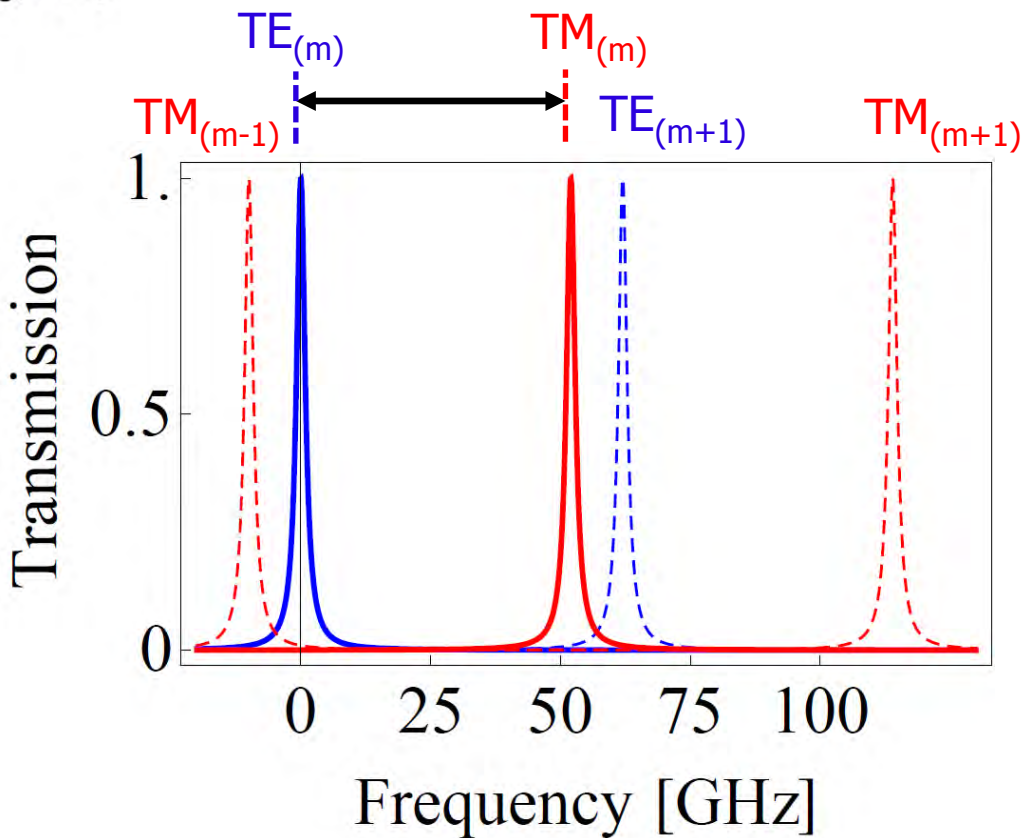
$$\omega_{TM} > \omega_{TE}$$

Role of geometric birefringence



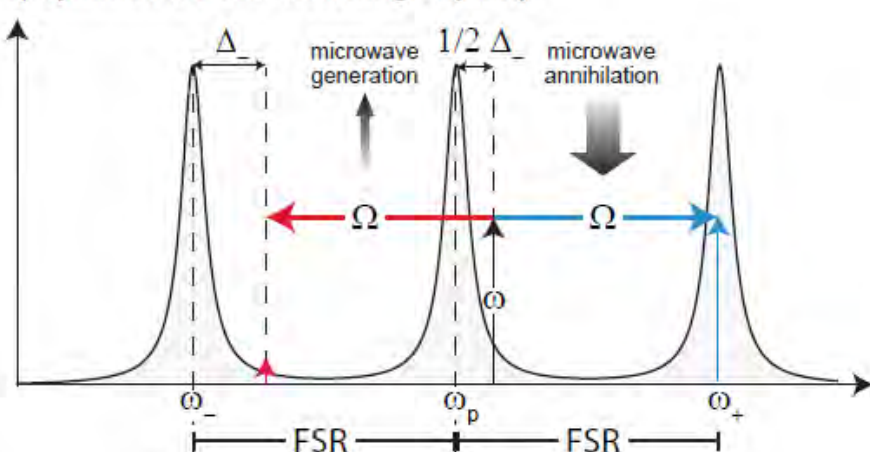
Geometrical birefringence

$$\text{FSR} \times \sqrt{1 - \frac{1}{m^2}}$$

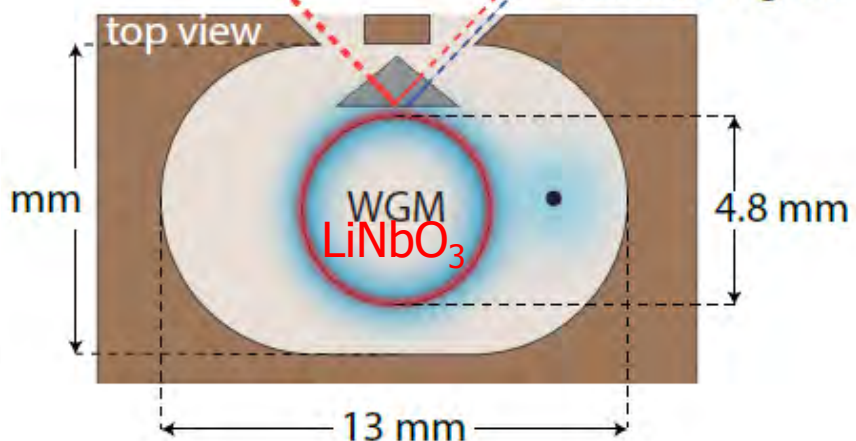


Microwave-light conversion via electro-optical WGM resonator

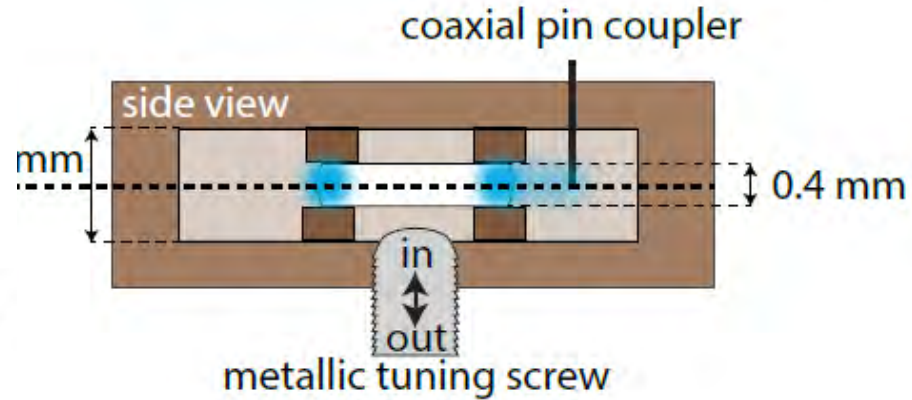
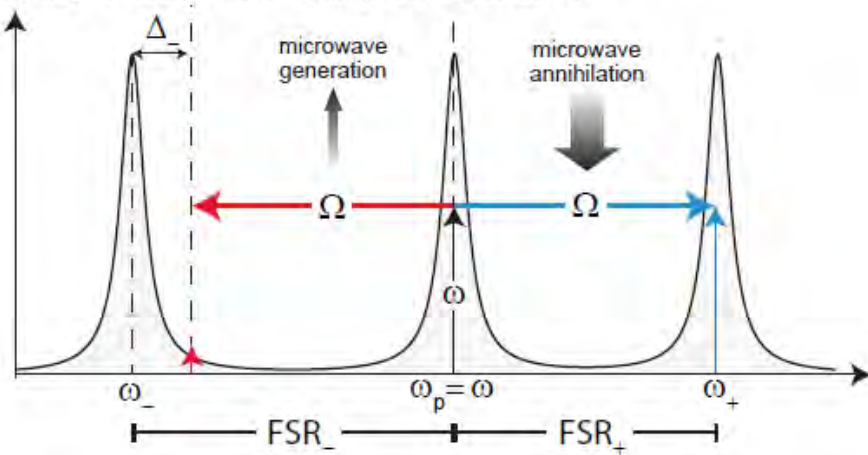
a) symmetric FSR - detuning of pump



pump
top view
reflected pump
sideband signal



b) asymmetric FSR - pump on resonance



Conversion efficiency $\sim 10^{-3}$

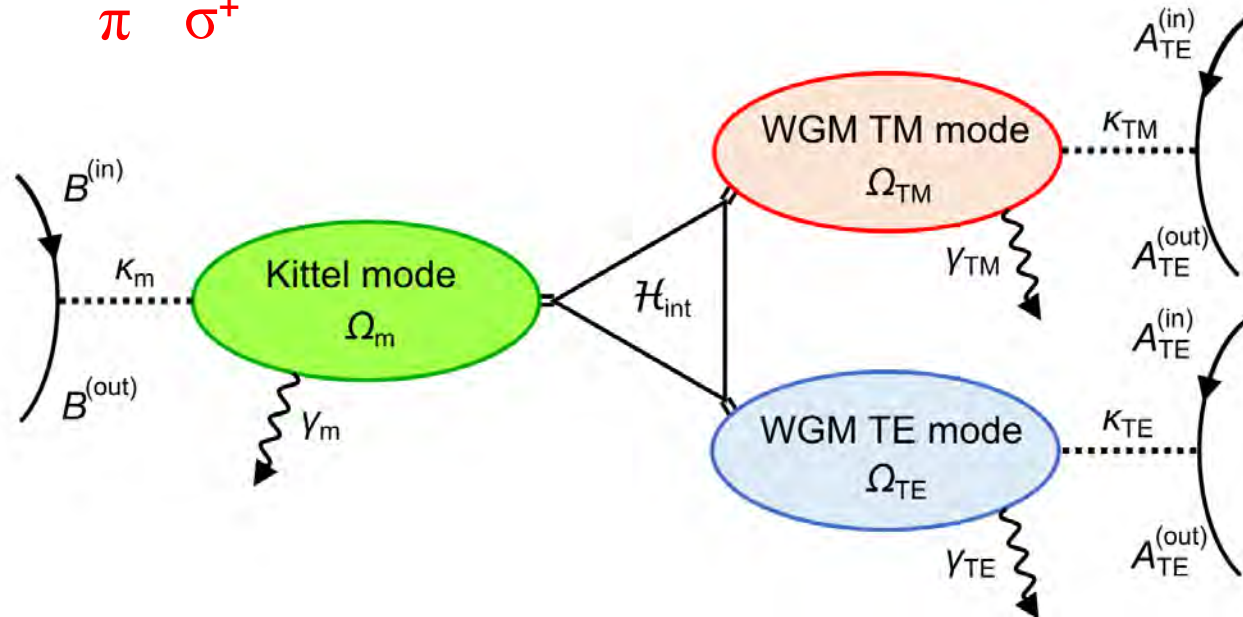
Model

$$\mathcal{H} = \hbar\Omega_{TE}a_{TE}^\dagger a_{TE} + \hbar\Omega_{TM}a_{TM}^\dagger a_{TM} + \hbar\Omega_m b^\dagger b$$

$$+ \hbar g(a_{TE}a_{TM}^\dagger b + a_{TE}^\dagger a_{TM} b^\dagger)$$

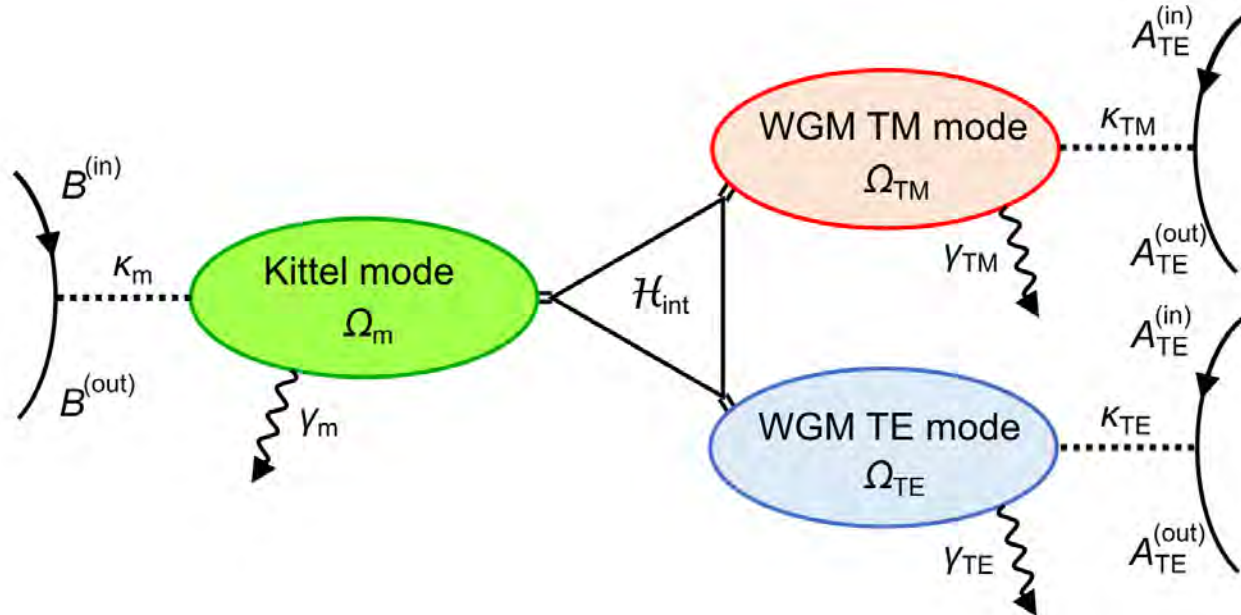
π σ^+

$$\delta = \omega_{TM} - \omega_{TE} - \omega_m = 0$$



$$n_{TM}^{(out)} = g^2 \frac{\kappa_{TE}}{\Delta_{TE}^2 + (\Gamma_{TE}/2)^2} \frac{\kappa_{TM}}{\Delta_{TM}^2 + (\Gamma_{TM}/2)^2} \frac{\kappa_m}{\Delta_m^2 + (\Gamma_m/2)^2} n_{TE}^{(in)} n_{MW}^{(in)}$$

Possible optimization



$$n_{\text{TM}}^{(\text{out})} = g^2 \frac{\kappa_{\text{TE}}}{\Delta_{\text{TE}}^2 + (\Gamma_{\text{TE}}/2)^2} \frac{\kappa_{\text{TM}}}{\Delta_{\text{TM}}^2 + (\Gamma_{\text{TM}}/2)^2} \frac{\kappa_m}{\Delta_m^2 + (\Gamma_m/2)^2} n_{\text{TE}}^{(\text{in})} n_{\text{MW}}^{(\text{in})}$$

- Set all detuning to zero, $\Omega_{\text{TM}} - \Omega_{\text{TE}} - \Omega_m = 0$ x7000
 - Make a better cavity x3500
 - Reduce sample volume x100

→ Conversion efficiency $\sim 1 \times 10^{-3}$ +Larger g \propto Verdet const.

Conclusions

Quantum magnonics with ferromagnet

- Strong coupling with superconducting qubit
- Vacuum Rabi oscillations
- Magnon-number-resolving spectroscopy

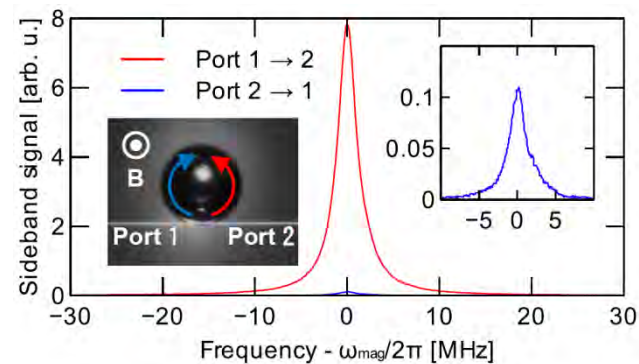
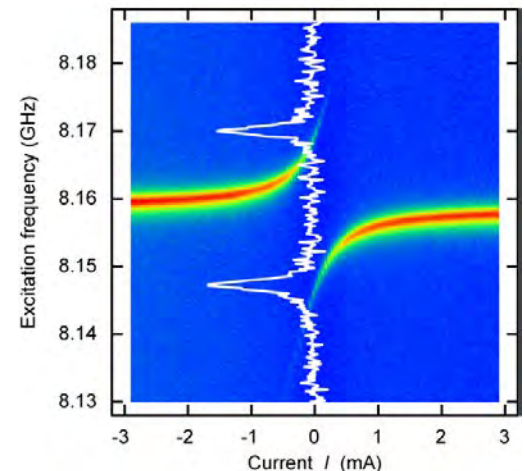


Optomagnonics

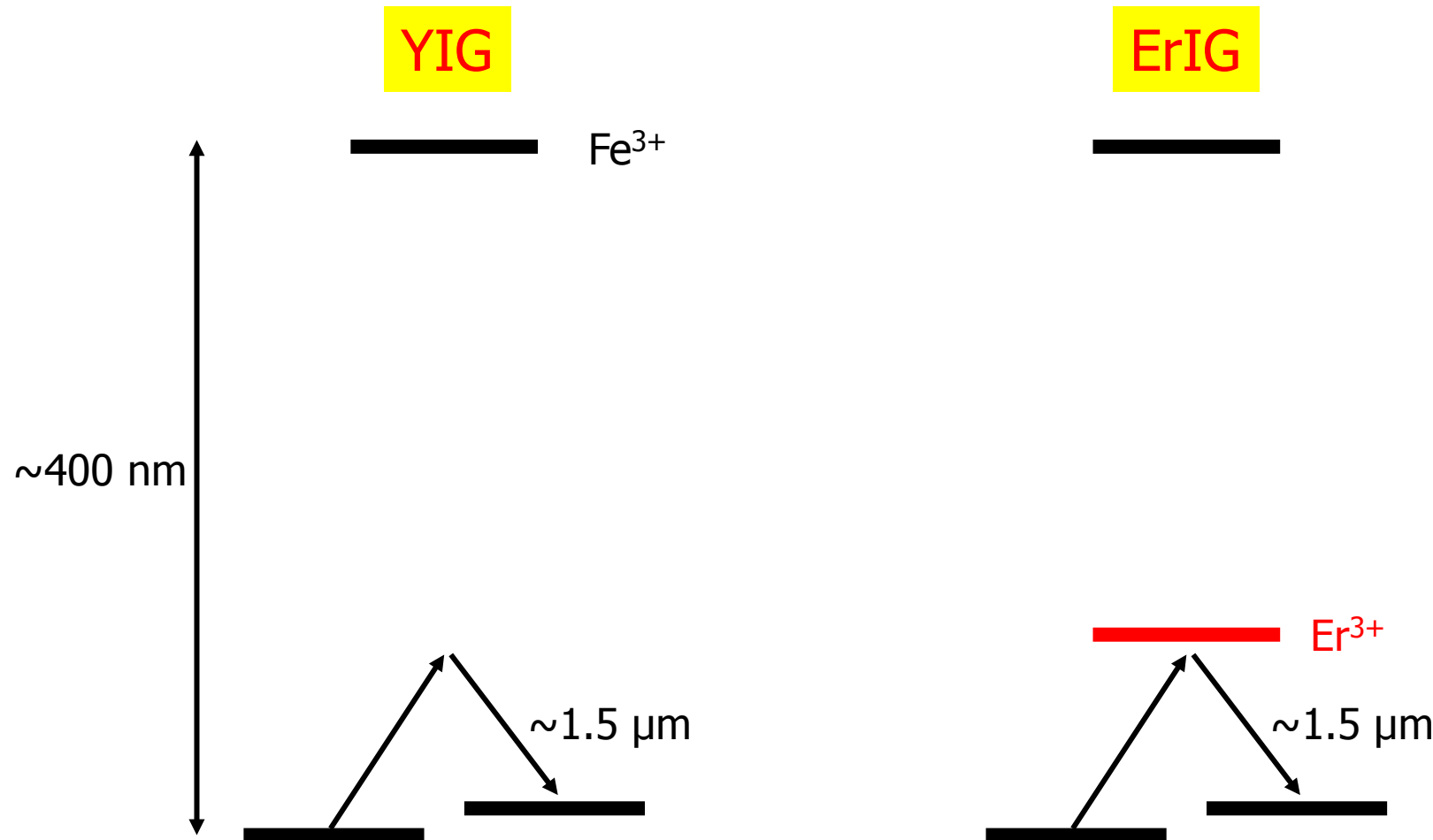
- Microwave-light conversion
- Cavity optomagnonics with WGM

In progress

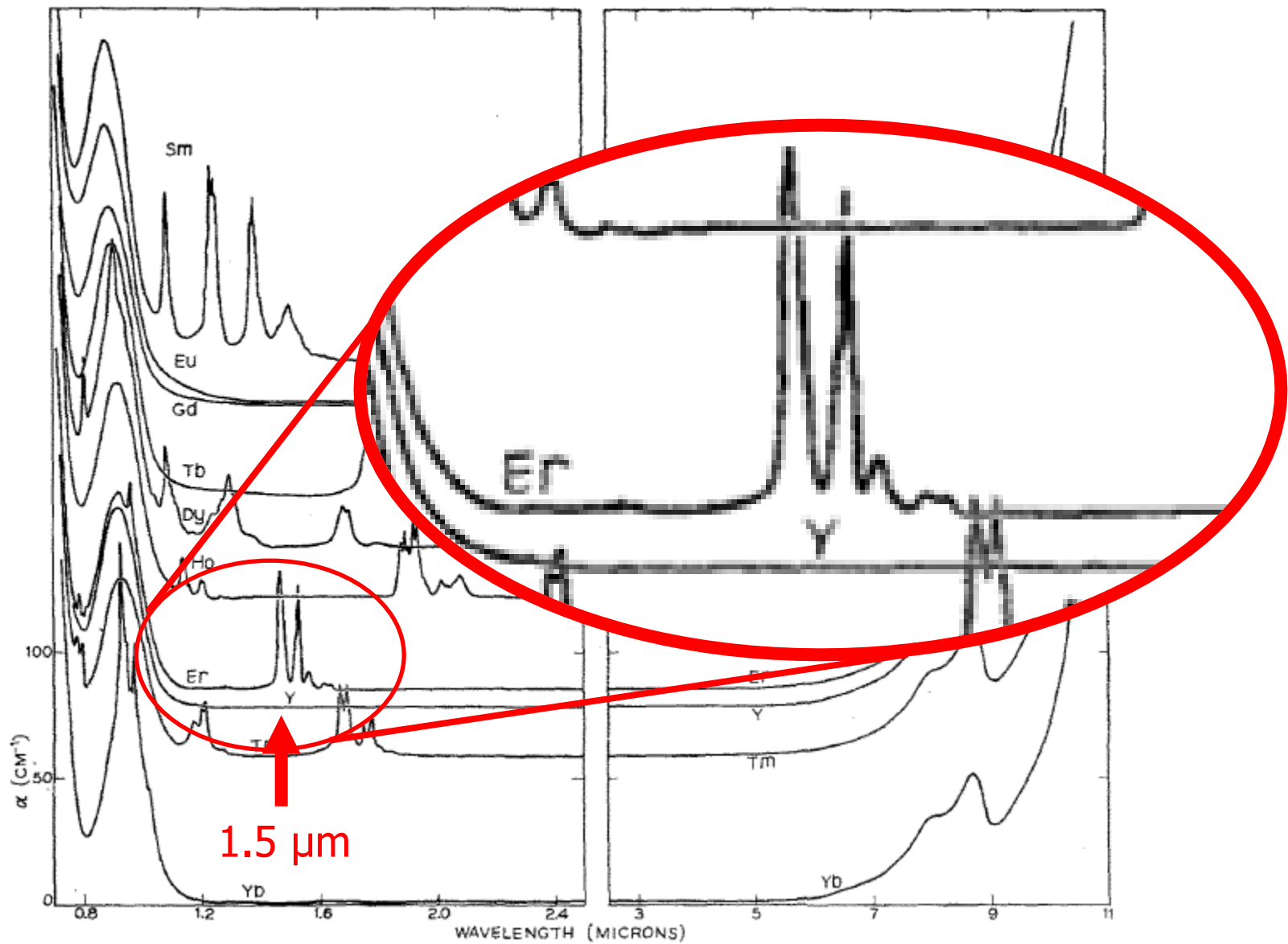
- Manipulation and measurement of non-classical states of magnon mode
- Optimization of optical coupling
- ErIG instead of YIG



Optical transitions in Yttrium and Erbium iron garnet



Optical absorption of REIG



Wood and Remeika, JAP 38, 1038 (1967) Bell Lab

Faraday rotation in ErIG

